2019 Spring

"Phase Equilibria *in* Materials"

05.29.2019

Eun Soo Park

Office: 33-313
Telephone: 880-7221
Email: espark@snu.ac.kr
Office hours: by an appointment

Chapter 14. The Association of Phase Regions

14.1. Law of adjoining phase regions

* Construction of phase diagram:

Phase rule ~ restrictions on the disposition of the phase regions

e.g. no two single phase regions adjoin each other through a line.

* Rules for adjoining phase regions in ternary systems

1) Masing, "a state space can ordinarily be bounded by another state space only if the number of phases in the second space is one less or one greater than that in the first space considered."

2) **Law of Adjoining Phase Regions: "most useful rule"**

$$\boxed{R_1 = R - D^- - D^+ \geq 0}$$

R_1 : Dimension of the boundary between neighboring phase regions

R : Dimension of the phase diagram or section of the diagram (vertical or isothermal)

D^- : the number of phases that disappear in the transition from one phase region to the other

D^+ : the number of phases that appear in the transition from one phase region to the other

14.2. Degenerate phase regions

* Law of adjoining phase region ~ applicable to <u>space model and their vertical and isothermal sections</u>, but <u>no "invariant reaction isotherm" or "four-phase plane" was included.</u>

* In considering phase diagrams or section containing degenerate phase regions, it is necessary to replace the missing dimensions before applying the law of adjoining phase regions.

Phase rule: invariant reaction (f=0)

$(p+f = c+1;\ 2+f = 1+1)$

Law of adjoining phase regions

$-1\ (R = 1,\ D^- = 1,\ D^+ = 1;$ therefore $R_I = -1)$

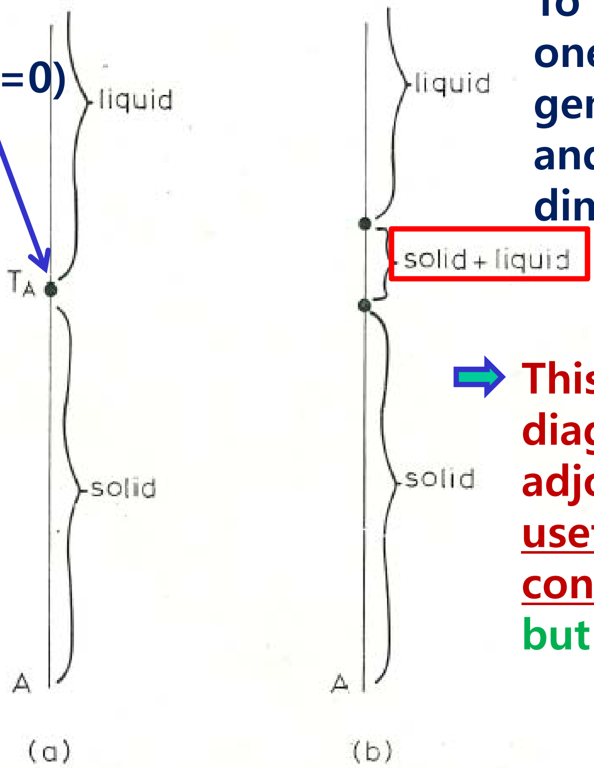

To overcome this situation, one regards the point T_A as a degenerate (liquid+solid) phase region and one replaces the missing dimension to give the diagram.

➡ This is now a topologically correct diagram which obeys the law of adjoining phase regions (<u>a very useful method for checking the construction of phase diagrams</u>) but lead to violation of phase rule.

Fig. 228. Illustration of a degenerate phase region. (a) The melting of pure A; (b) the melting of pure A when point T_A is regarded as a degenerate phase region and replaced by a "solid+liquid" phase region.

*** Degenerate phase regions in space models of phase diagrams and in their sections can be dealt with in a similar manner by replacing the missing dimensions.**

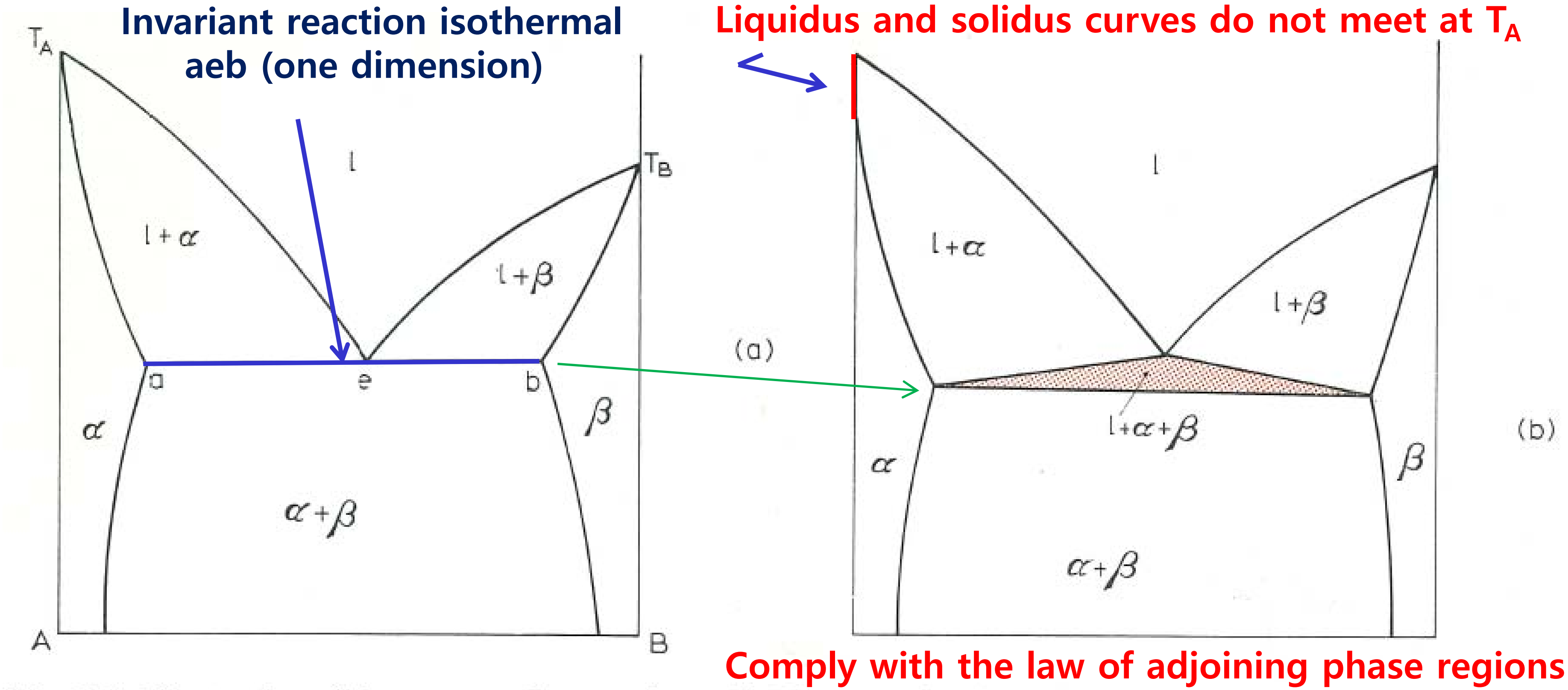

Fig. 229. Illustration of degenerate phase regions. (a) The eutectic phase diagram; (b) corresponding diagram allowing for degeneration of the phase regions.

(b) R=2; R_1=0_only four lines may meet at a point in two-dimensional diagrams

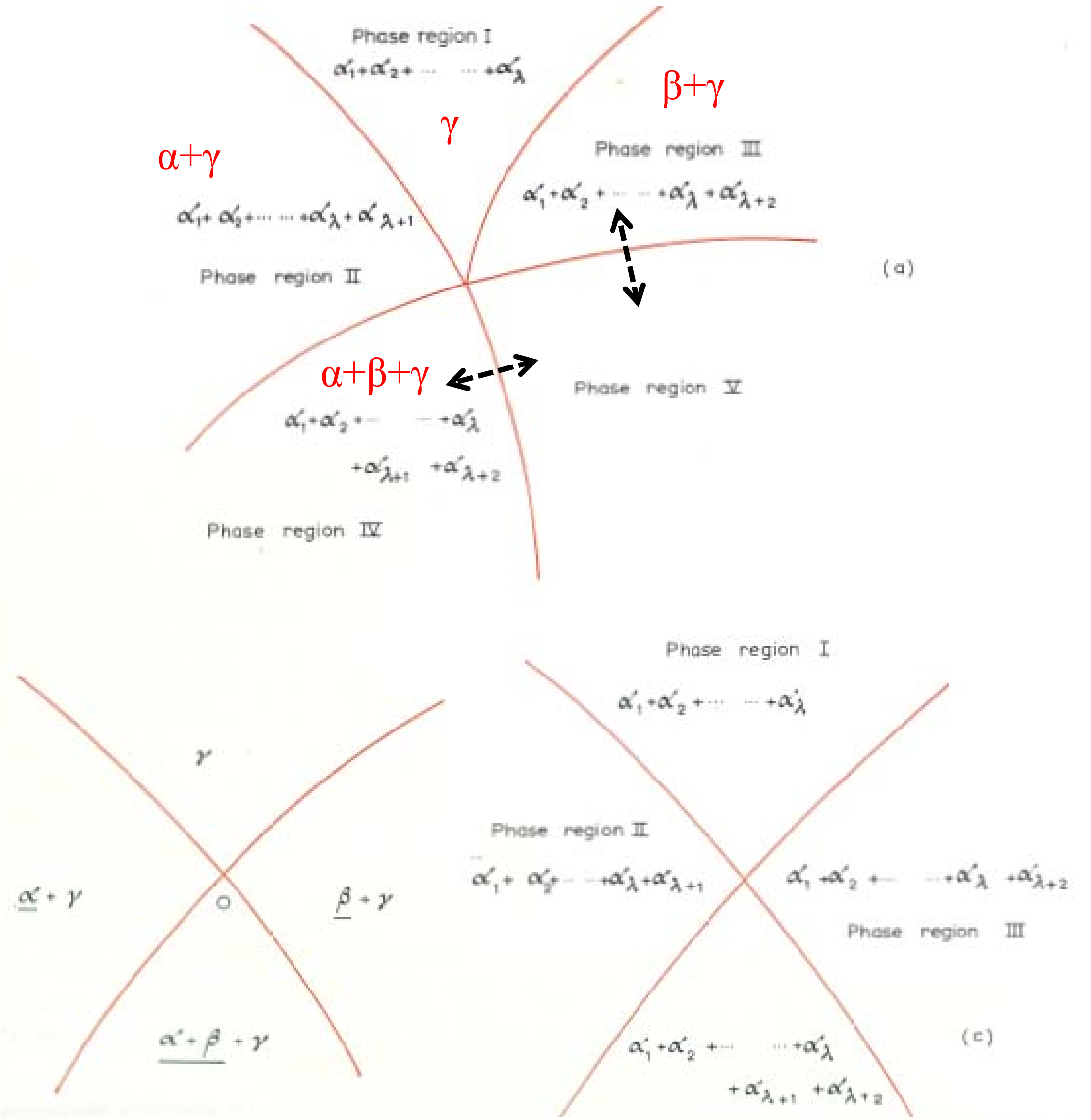

Fig. 233. Boundary lines meeting at a point in a two-dimensional diagram. (a) Impossibility of five lines meeting at a point; (b) distribution of phase regions when four lines meet at a point; (c) only four lines may meet at a point.

That there are exceptions to the rule that four lines meet at a point in a two-dimensional diagram is evident from an examination of Fig. 178b and f. In each case six lines meet at a central point. It will be noted, however, that in both cases the section passes through an invariant point—*E* and *c* respectively. Palatnik and Landau call such sections nodal or non-regular sections. Only regular sections obey the law of adjoining phase regions completely.

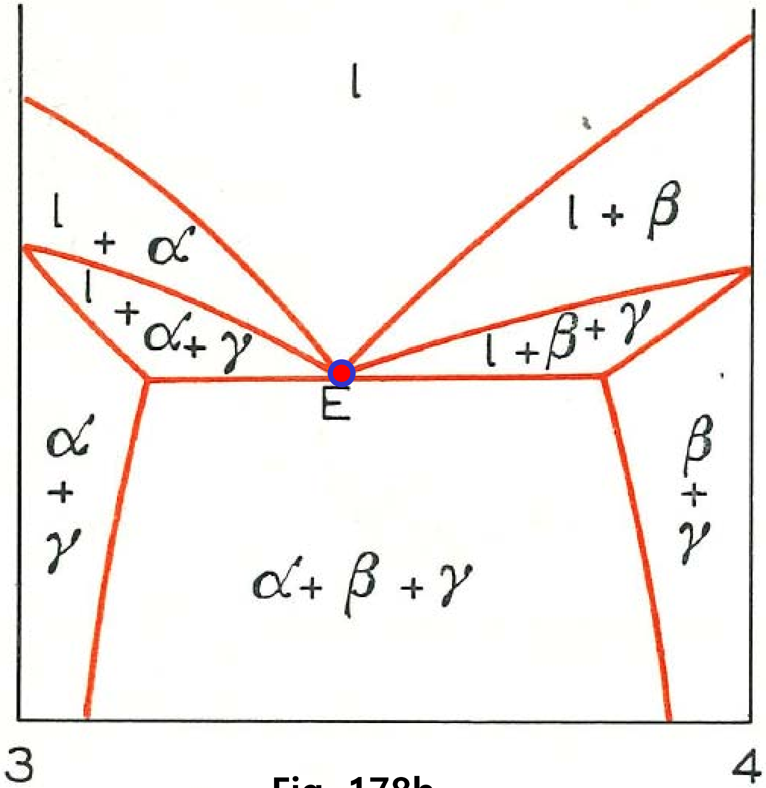

Fig. 178b

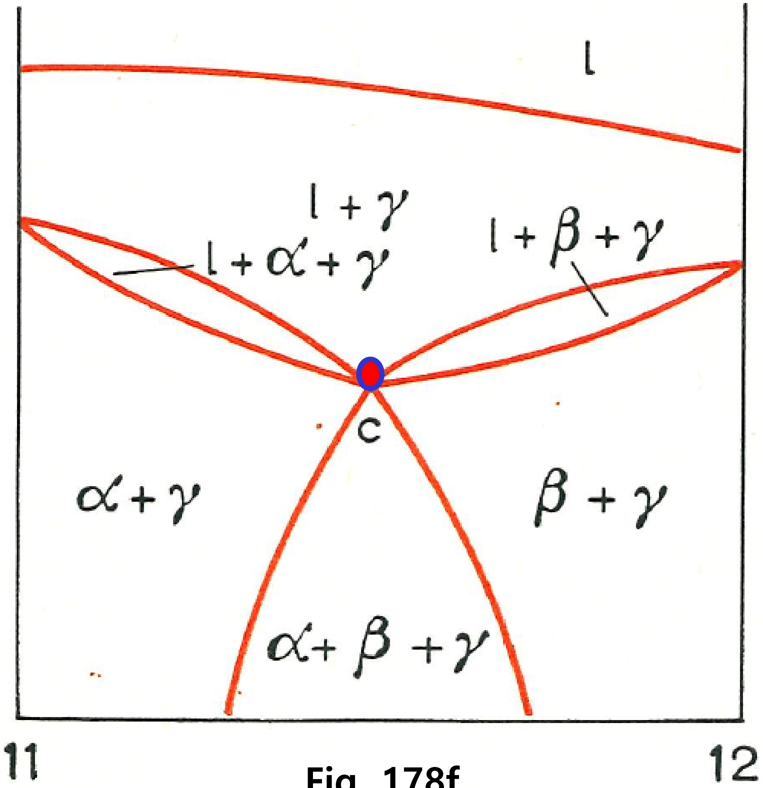

Fig. 178f

14.5. Non-regular two-dimensional sections

Nodal plexi can be classified into four types according to the manner of their formation:

Type 1 The nodal plexus is formed without degeneration of any geometrical element of the two-dimensional regular section to elements of a lower dimension

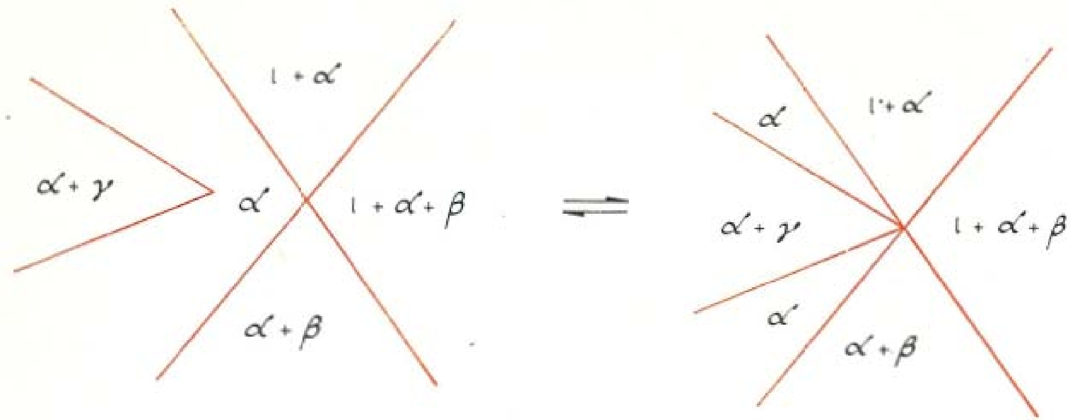

Fig. 235. Type 1 nodal plexus.

Type 2 The number of lines degenerate to a point but there is no degeneration of two dimensional phase regions. In the formation of a type 2 nodal plexus the line O_1O_2 in the regular section degenerates into point O of the nodal plexus associated with the non-regular section.

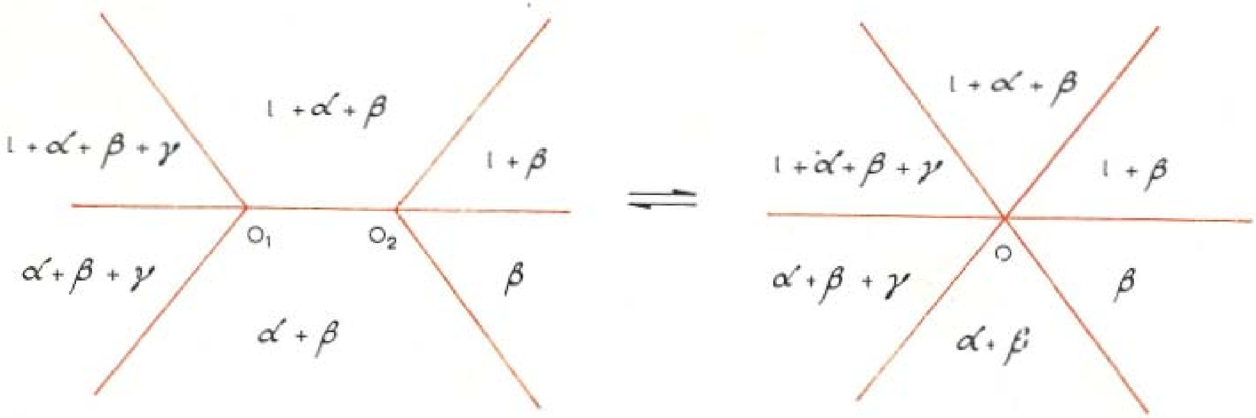

Fig. 236. Type 2 nodal plexus.

14.5. Non-regular two-dimensional sections

Nodal plexi can be classified into four types according to the manner of their formation:

***Type* 3** **A number of two dimensional phase regions degenerate into a point. In this case the phase region $l + \alpha + \beta$ disappears with the transition from a regular to a non-regular two dimensional section.**

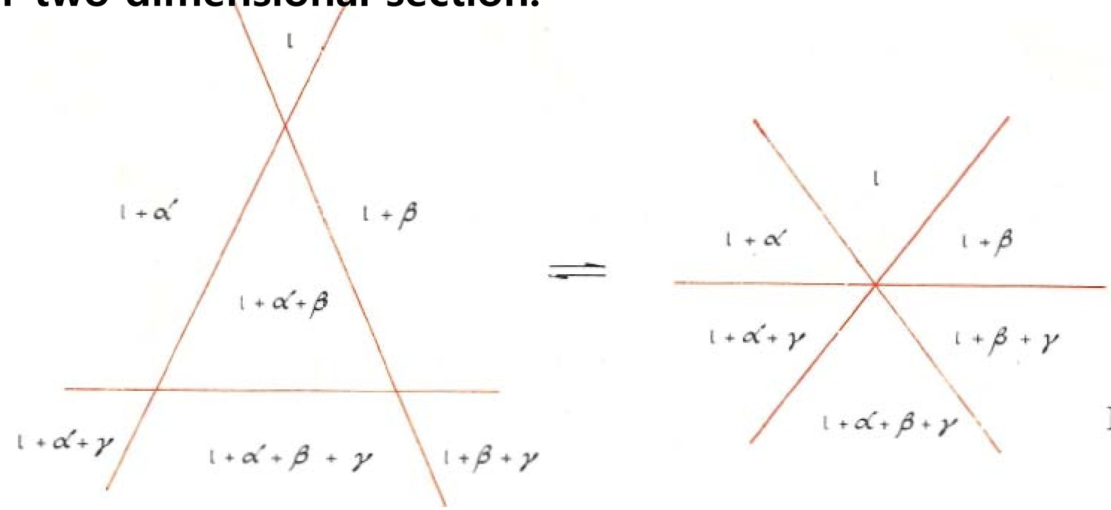

Fig. 237. Type 3 nodal plexus.

***Type* 4** **A number of two dimensional phase regions degenerate to a line. In the formation of the nodal plexus the phase region $l + \beta + \gamma$ and $\beta + \gamma$ have degenerated into the line O_1O_2.**

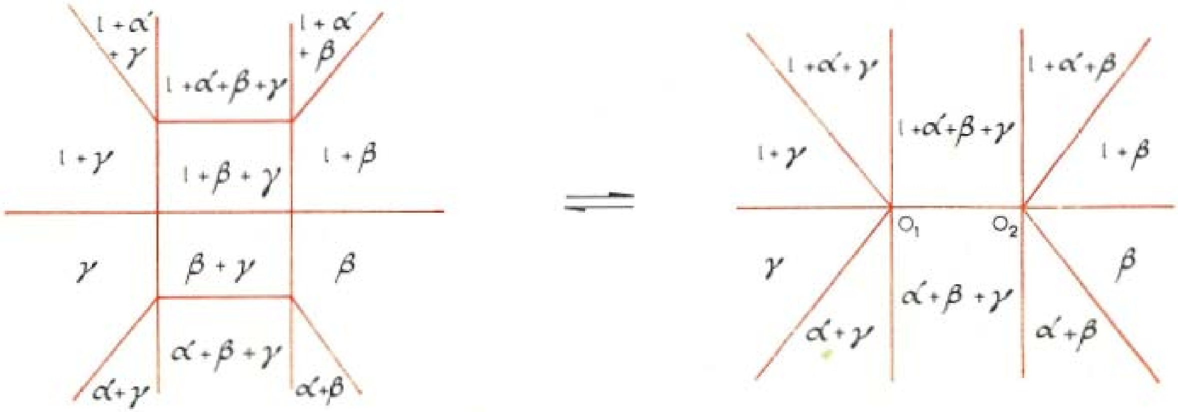

Fig. 238. Type 4 nodal plexus.

14.5. Non-regular two-dimensional sections

Nodal plexi can be classified into four types according to the manner of their formation:

Nodal plexi of mixed types may also be formed. A type 2/3 one is shown in Fig. 239. In the formation of the nodal plexus the two dimensional l + γ region degenerates to a point – triangle $O_2O_3O_4$ degenerates to point O – and the line O_1O_2 degenerates to the same point O. The former process corresponds to the formation of a type 3 nodal plexus and the latter to the formation of a type 2 nodal plexus.

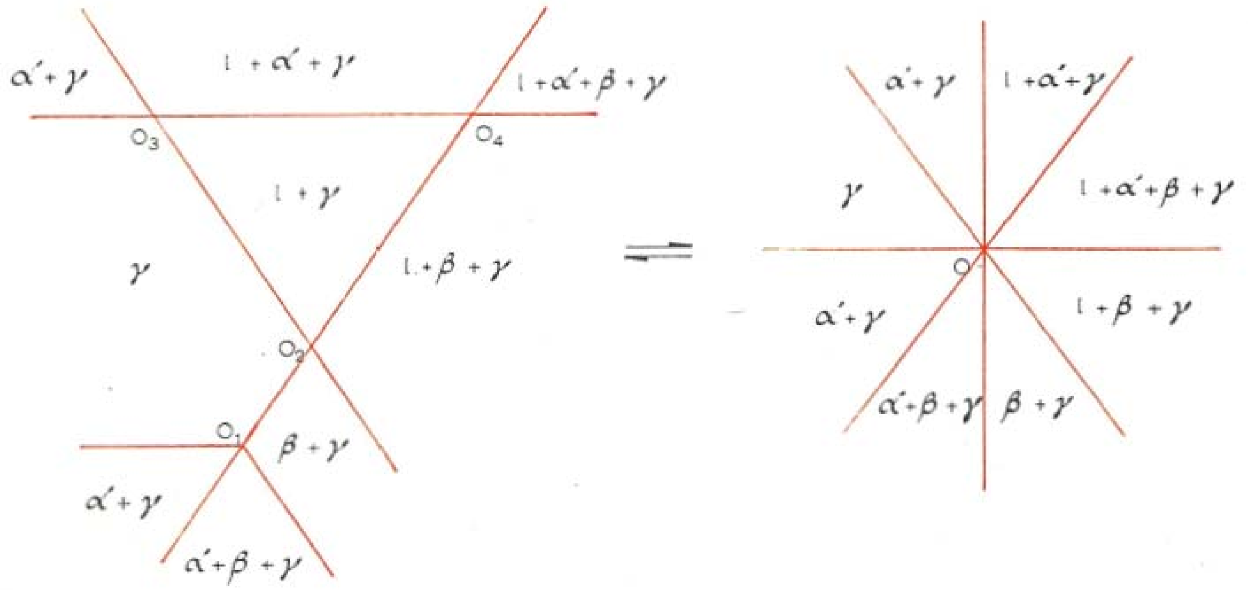

Fig. 239. Mixed type 2/3 nodal plexus.

1) **Formation of nodal plexi:**
   Transition from a regular section to a non-regular section of a ternary system

2) **Opening of nodal plexi:**
   Subsequent transition from the non-regular section back to a regular section

Fig. 240. Formation and opening of nodal plexi

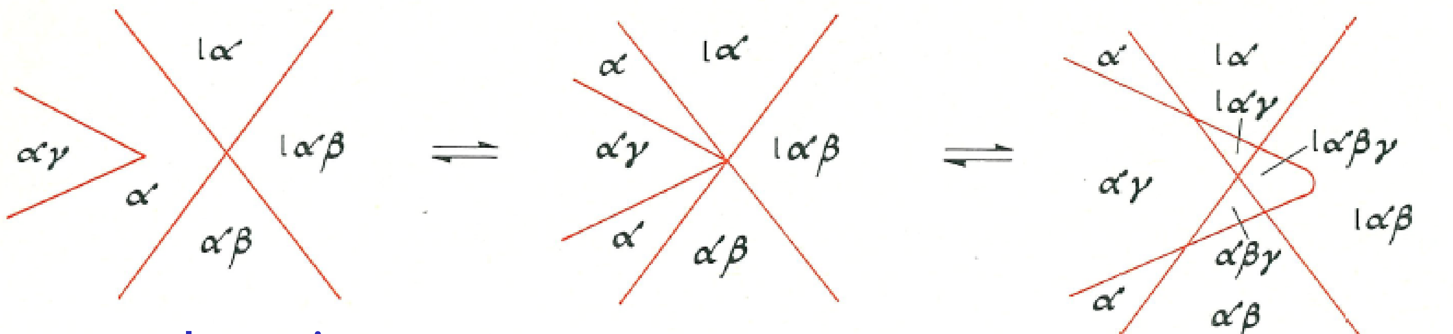

<regular section> <non-regular section> <regular section>

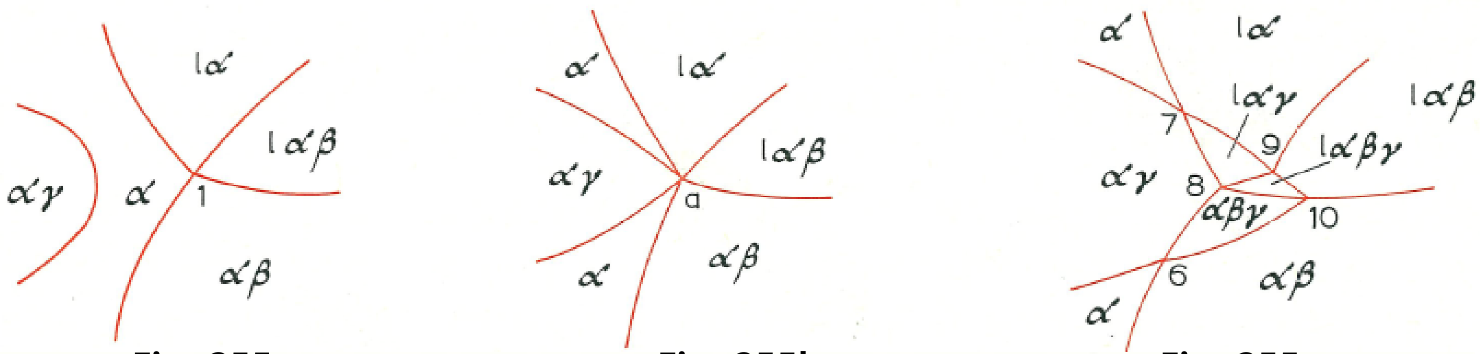

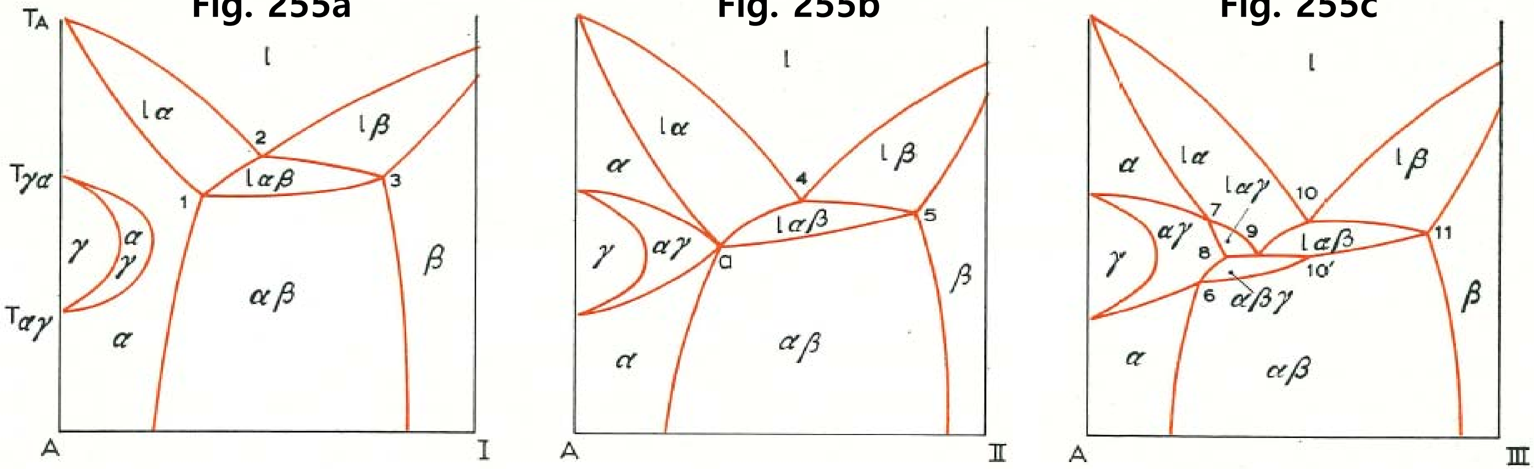

Fig. 255a Fig. 255b Fig. 255c

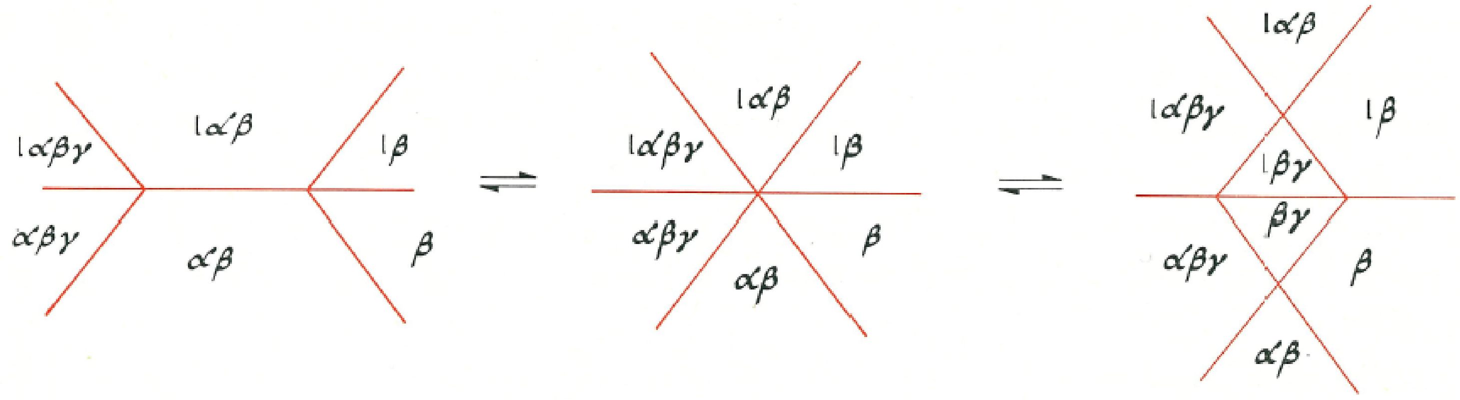

TYPE II →

← TYPE III

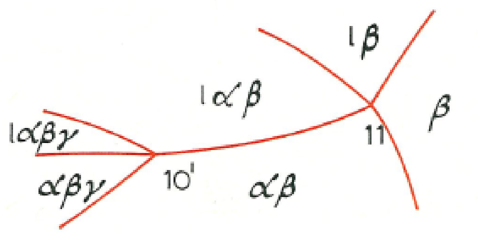

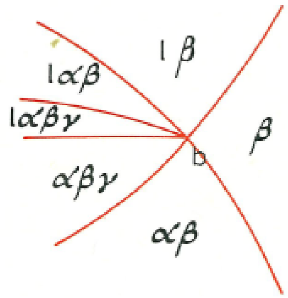

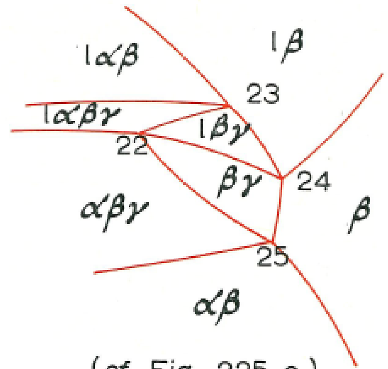

(cf. Fig. 225 c)

(cf. Fig. 225 d)

(cf. Fig. 225 e)

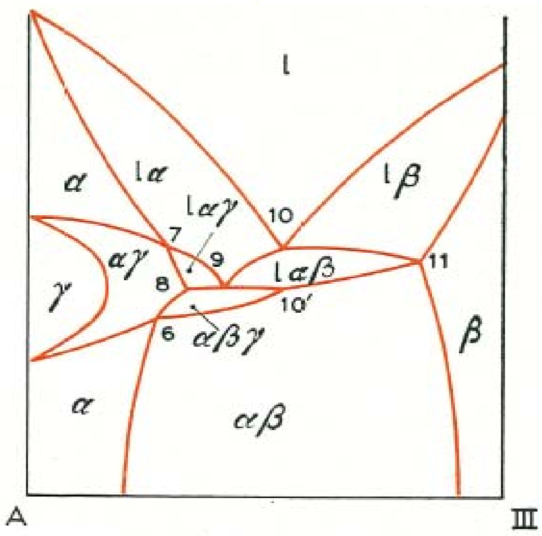

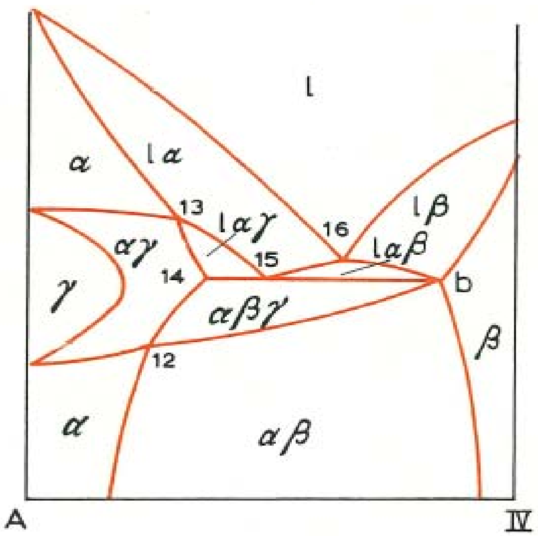

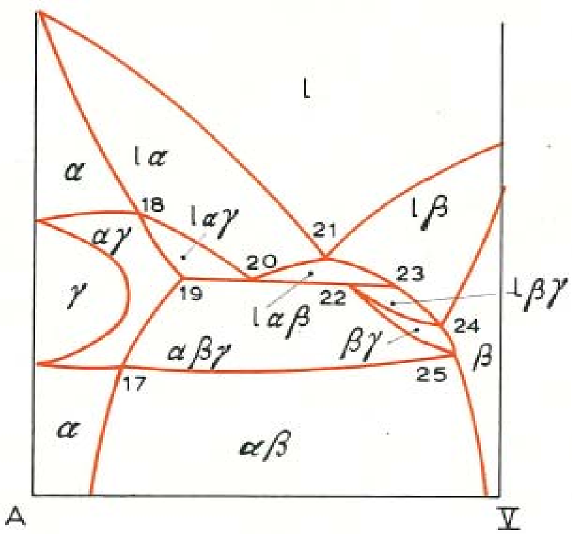

Formation | Nodal plexus | Opening

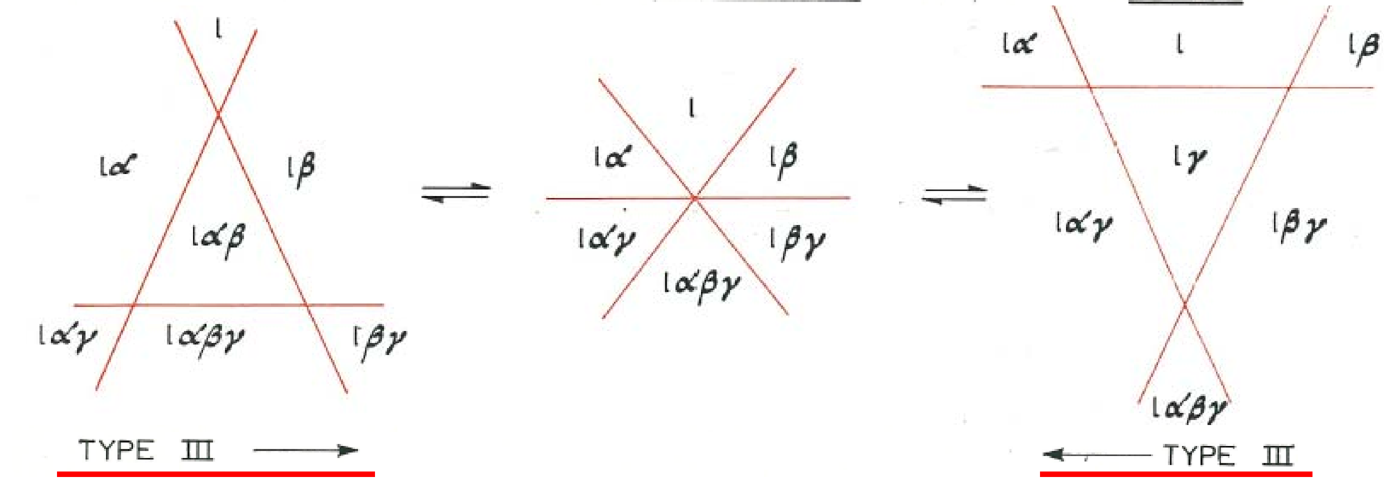

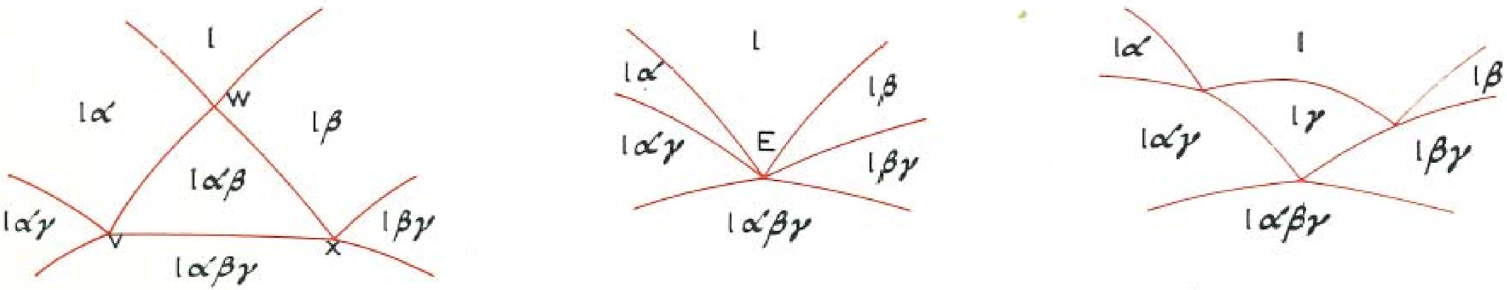

(cf. Fig. 178 a) | (cf Fig. 178 b) | (cf. Fig. 178 c)

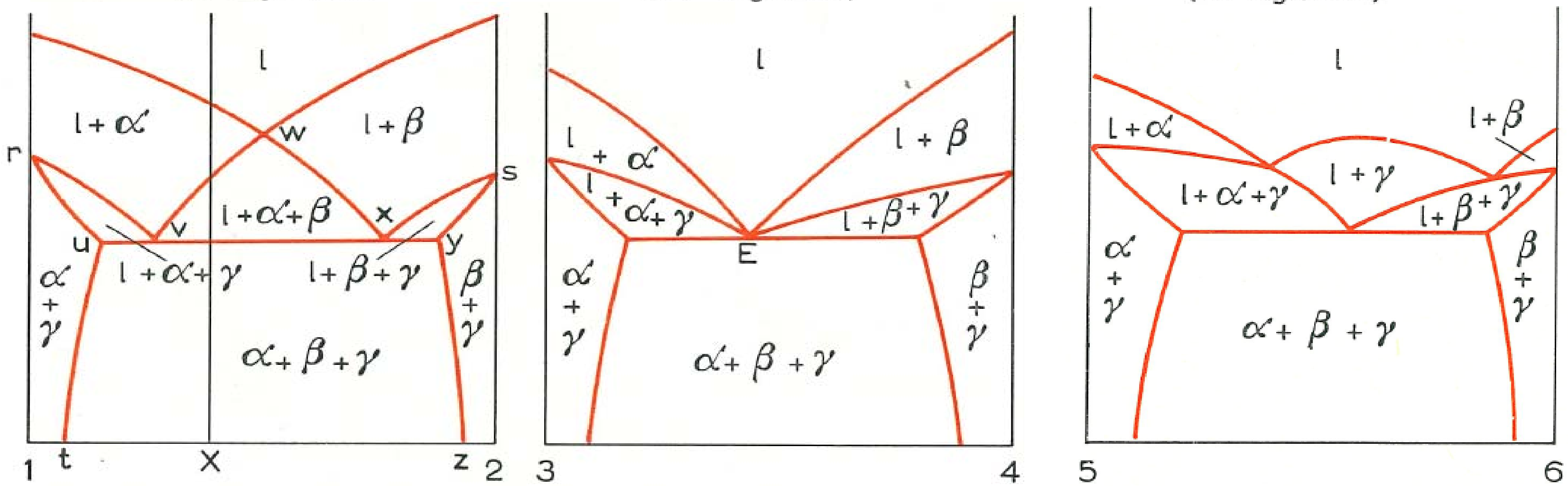

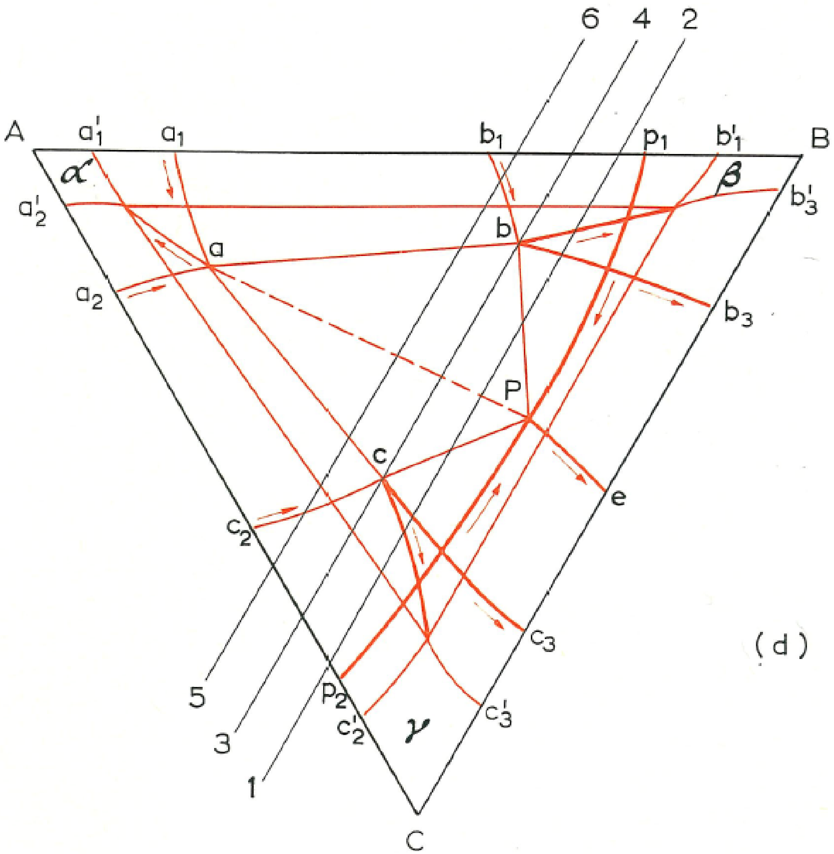
6 4 2
A
a_1'
a_1
b_1
p_1
b_1'
B
α
β
a_2'
b_3'
a
b
a_2
b_3
P
c
e
c_2
c_3
5
3
1
p_2
c_2'
γ
c_3'
C

(d)

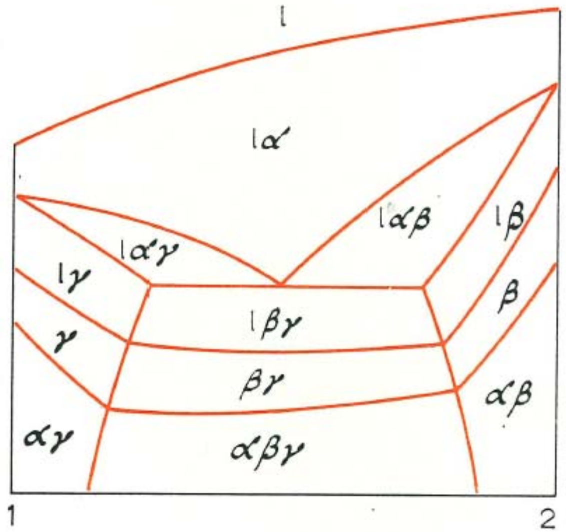
l
lα
lαβ
lβ
lαγ
lγ
β
lβγ
γ
βγ
αβ
αγ
αβγ
1
2

(a)

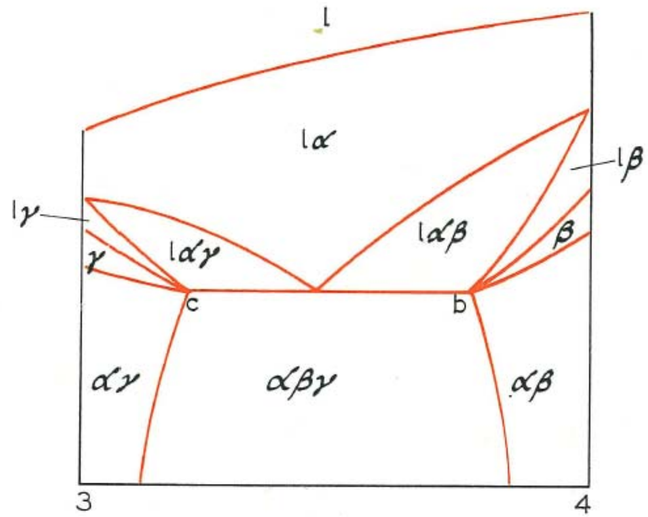
l
lα
lβ
lγ
γ
lαγ
lαβ
β
c
b
αγ
αβγ
αβ
3
4

(b)

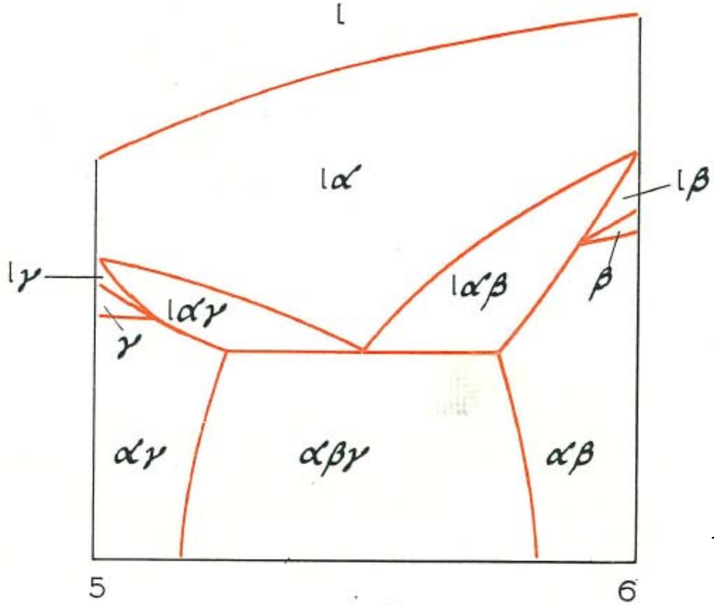
l
lα
lβ
lγ
lαγ
lαβ
β
γ
αγ
αβγ
αβ
5
6

(c)

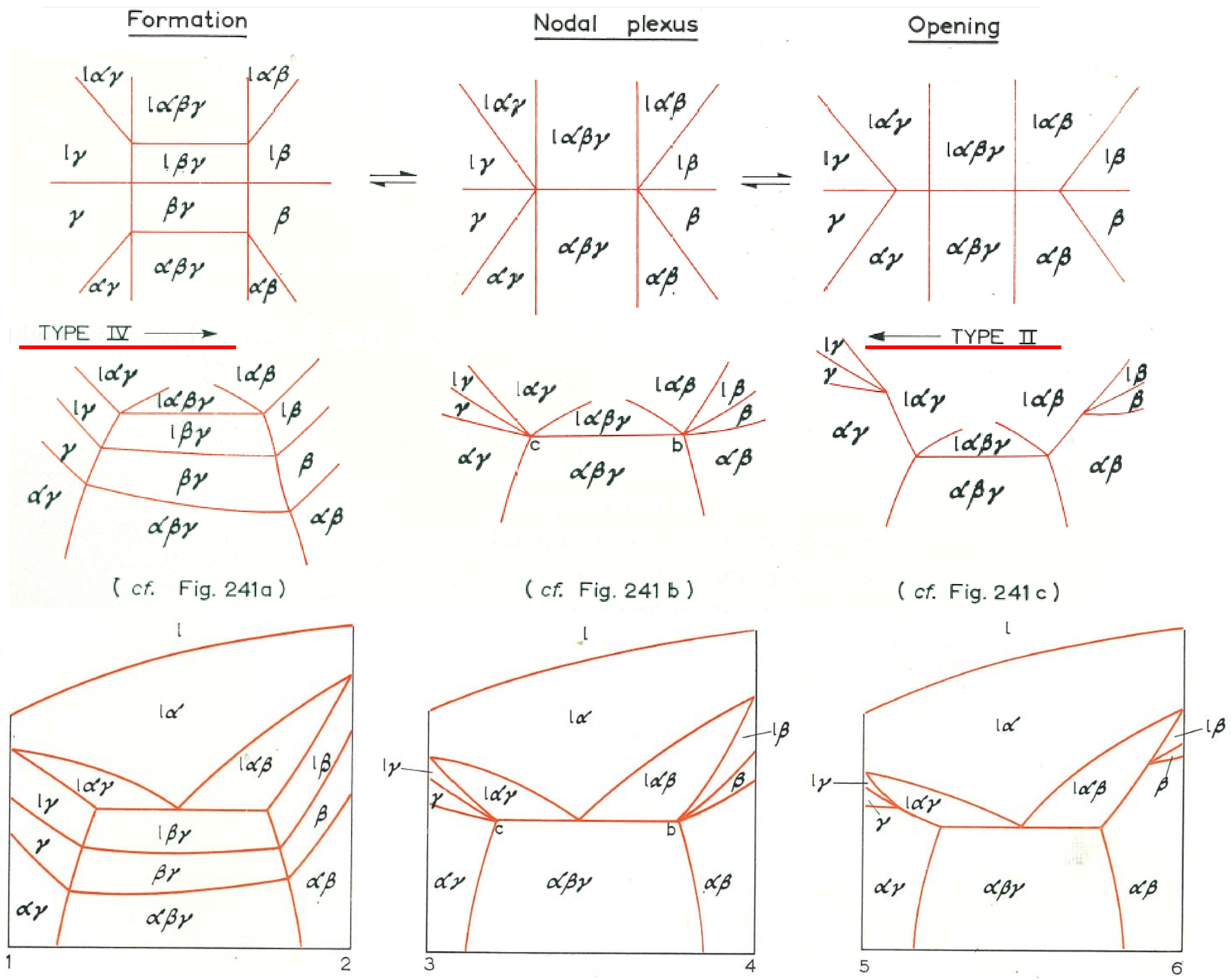
Formation
Nodal plexus
Opening
TYPE IV
TYPE II
(cf. Fig. 241a)
(cf. Fig. 241 b)
(cf. Fig. 241 c)
lα
lαβ
lαγ
lβγ
βγ
αβγ
lαβγ
lγ
lβ
γ
β
αγ
αβ
c
b
l
1
2
3
4
5
6

Fig. 240. Formation and opening of nodal plexi

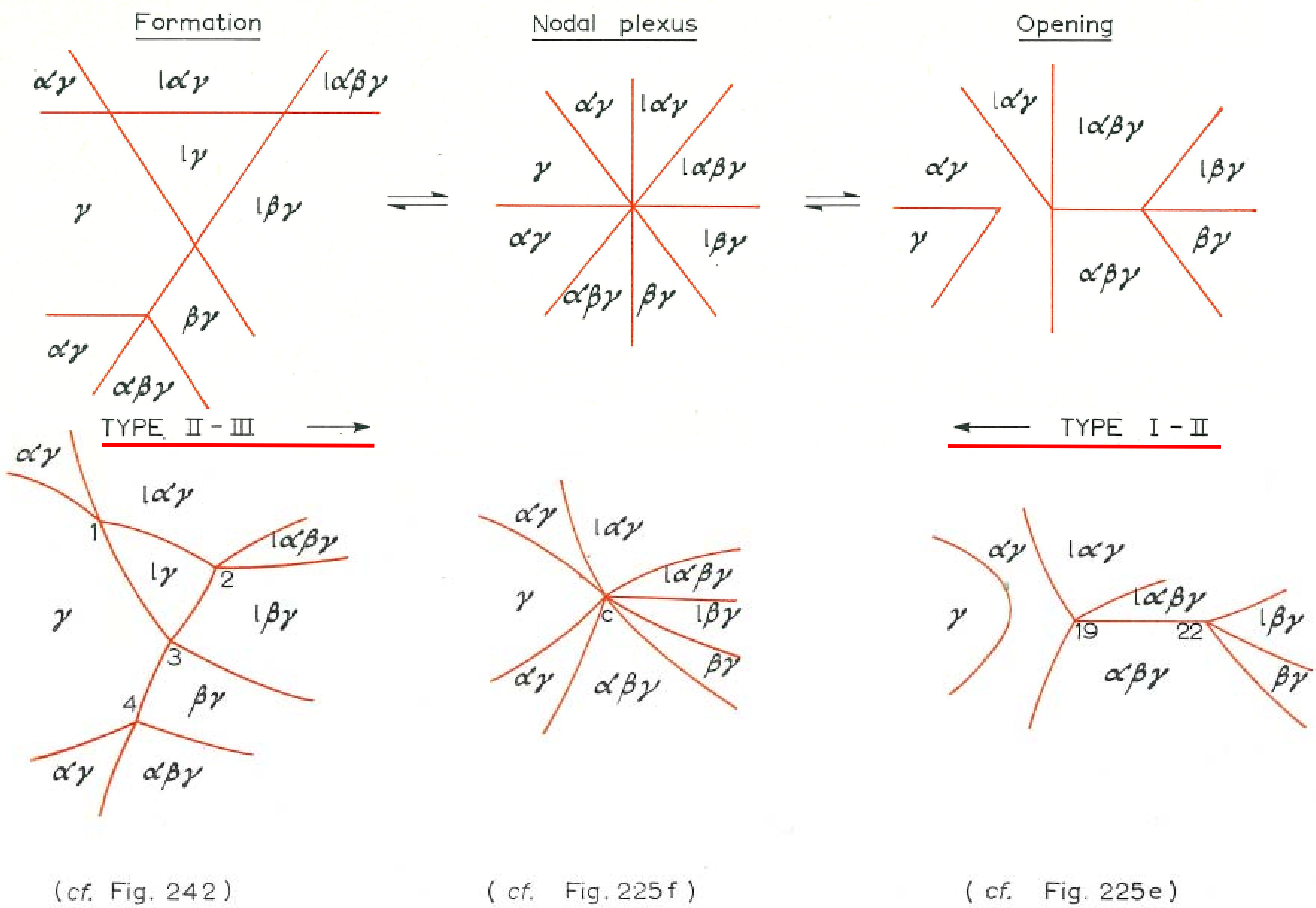

Fig. 240 (e).

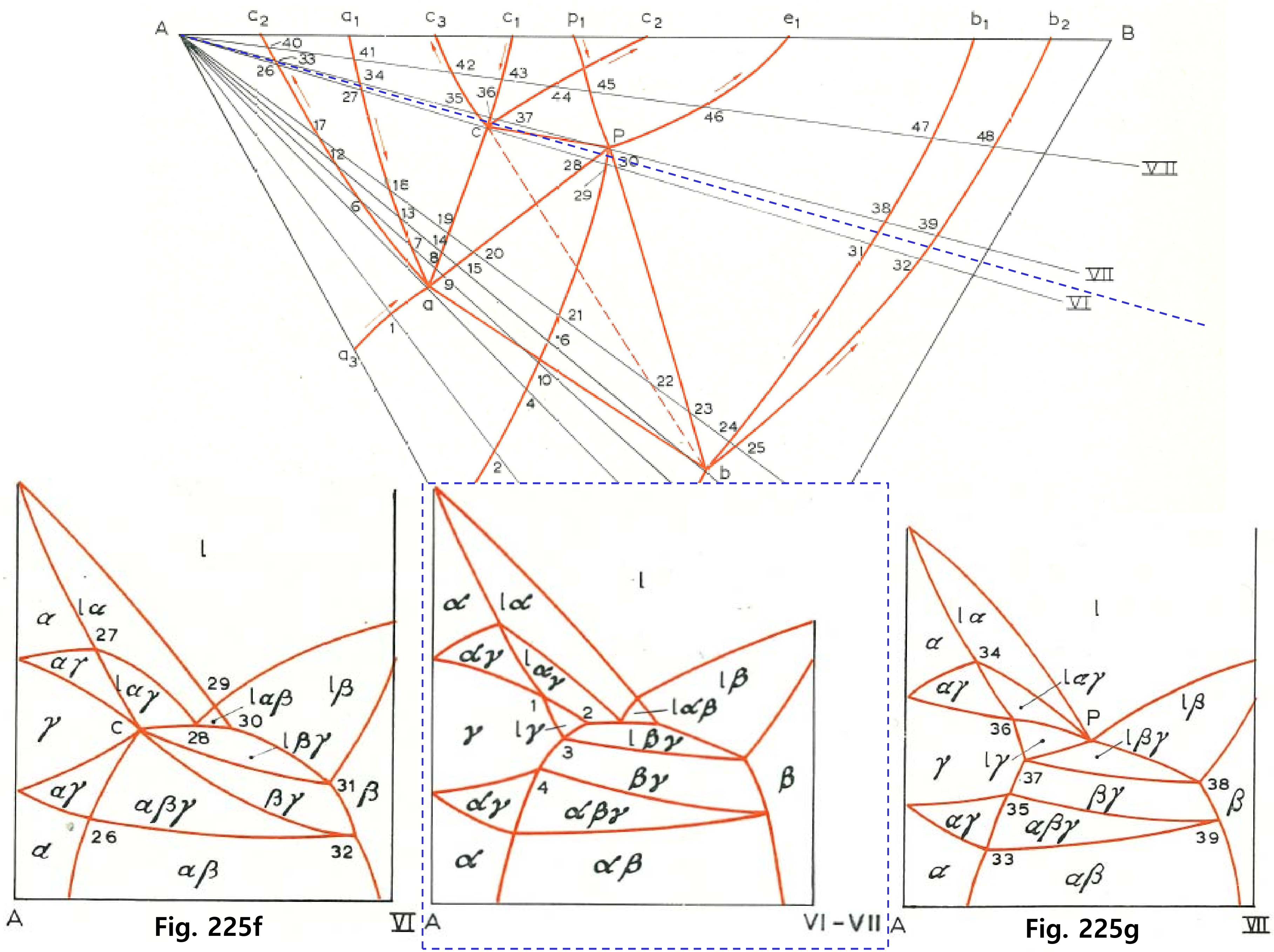

Fig. 242. Vertical section intermediate between Figs. 225f and g.

Fig. 240. Formation and opening of nodal plexi

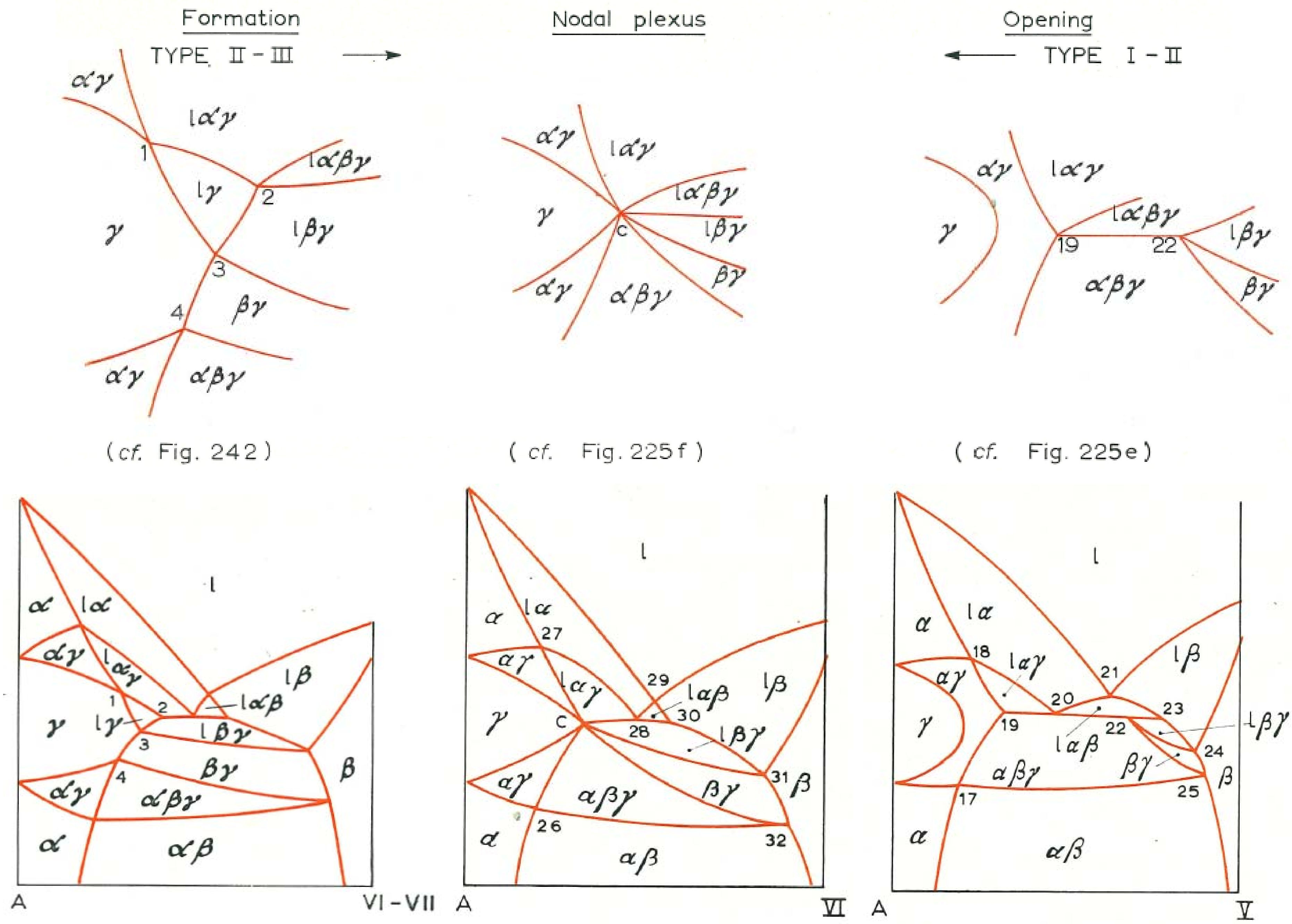

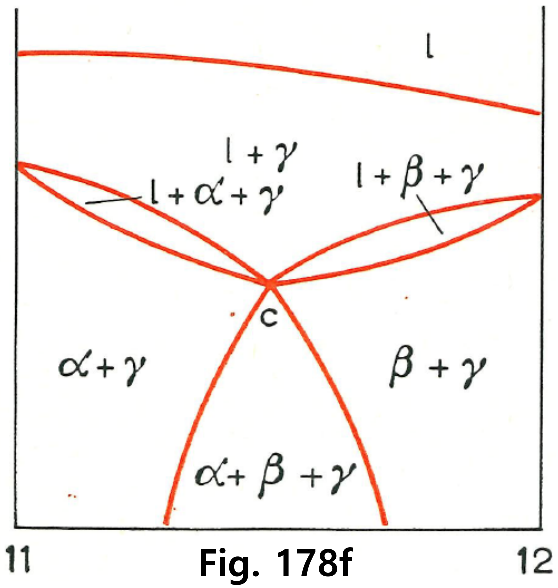

Fig. 178f

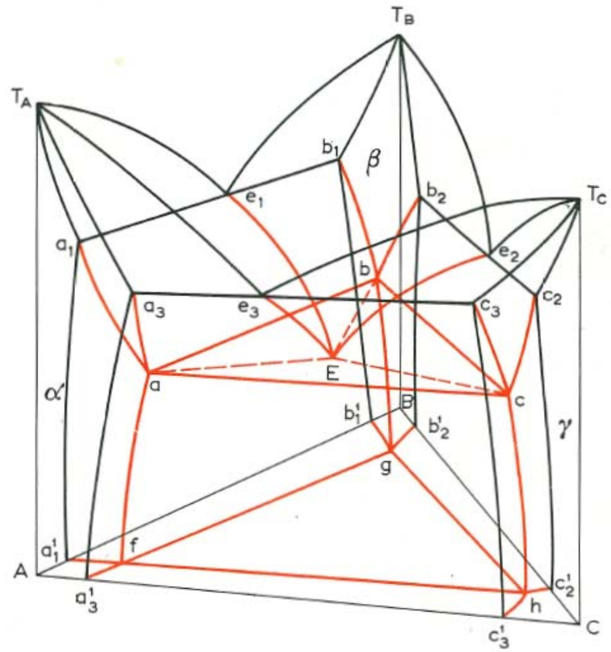

Fig. 173a

In general, the distribution of phases in non-regular sections does not obey the cross rule. Consider the non-regular section 11–12 through the invariant point c in Fig. 177. In the section (Fig. 178f) six lines meet at point c. Referring to the ternary space model in Fig. 173a, eight phase regions adjoin point c. These are:

(1) γ where c is a point on surface $T_C c_2 c_2^1 h c_3^1 c_3$
(2) $l+\gamma$ where c is a point on surface $T_C c_3 c c_2$
(3) $\alpha+\gamma$ where c is a point on surface $c_3 c h c_3^1$
(4) $\beta+\gamma$ where c is a point on surface $c_2 c h c_2^1$
(5) $l+\alpha+\gamma$ where c is a point on line $c_3 c$
(6) $l+\beta+\gamma$ where c is a point on line $c_2 c$
(7) $\alpha+\beta+\gamma$ where c is a point on line ch
(8) $l+\alpha+\beta+\gamma$ where c is a point representing one apex of the phase region.

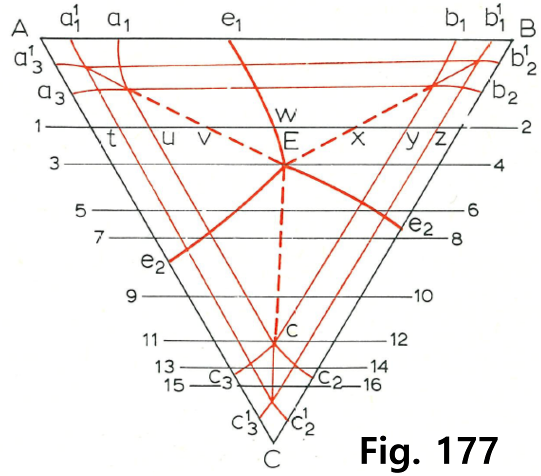

Fig. 177

Of these eight phase regions only six adjoin point c in the non-regular section (Fig. 178f). In the transition from the non-regular section to the regular sections which straddle it the other two phase regions will appear. These phase regions are the γ and the $l+\alpha+\beta+\gamma$ regions.

*** Three methods by which an non-regular section of the type shown in Fig. 178f may change to a regular section → Figs. 240a, b and c → "Figs. 240c is the only possible mode"**

Transition of the non-regular section (middle figure) into regular sections.

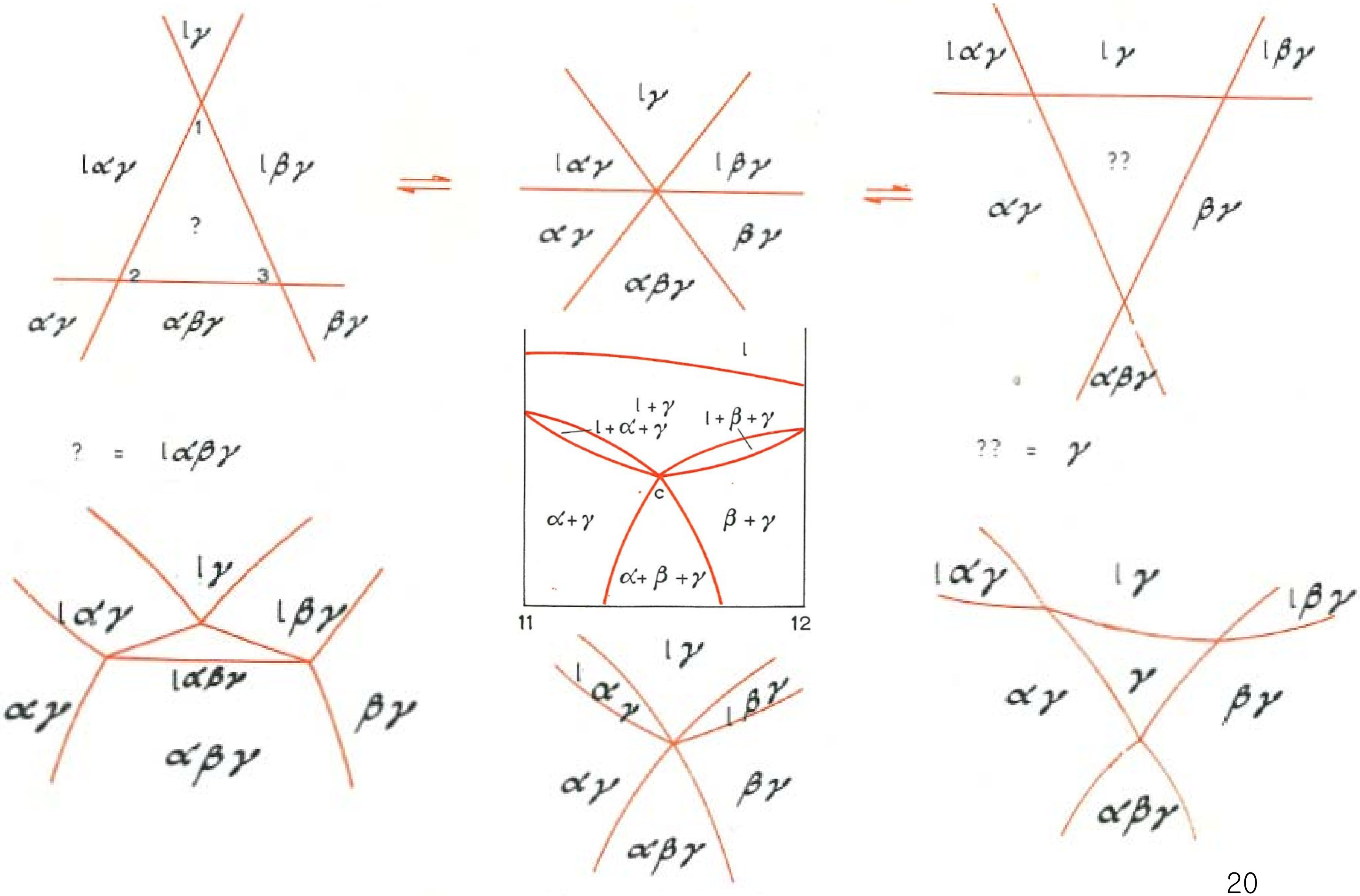

Corresponding vertical sections to Fig. 243.

“Figs. 240c is the only possible mode”

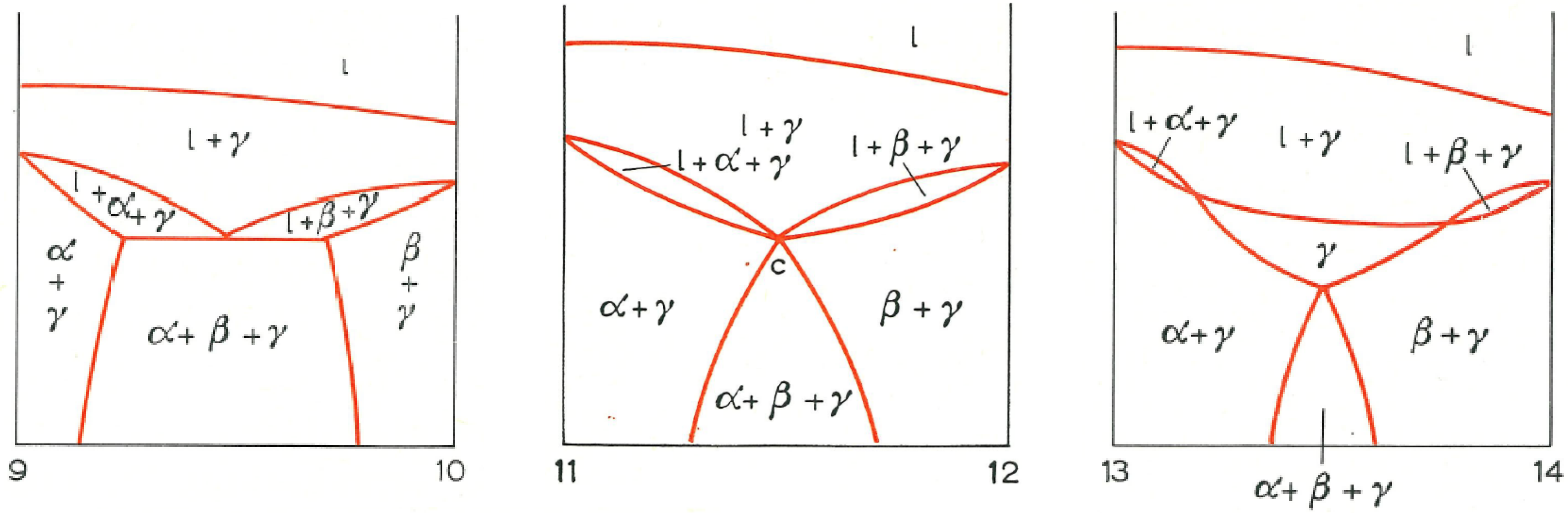

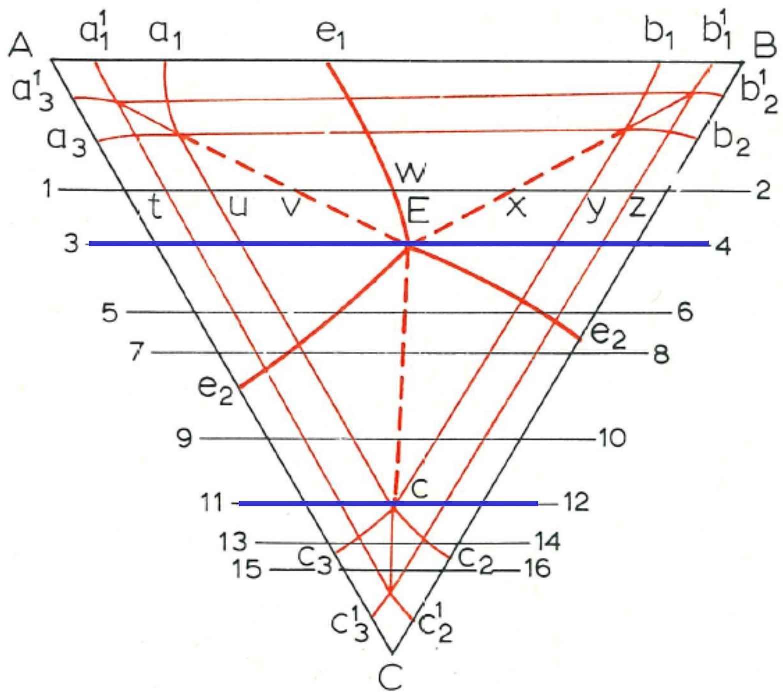

* The importance of non-regular sections lies in the fact that they represent an intermediate step in the transition from one-regular sections to another regular section. If we started with the two non-regular sections 11-12 and 3-4 passing through the invariant points c and E, we could construct the sequence of vertical section given in Fig. 178.

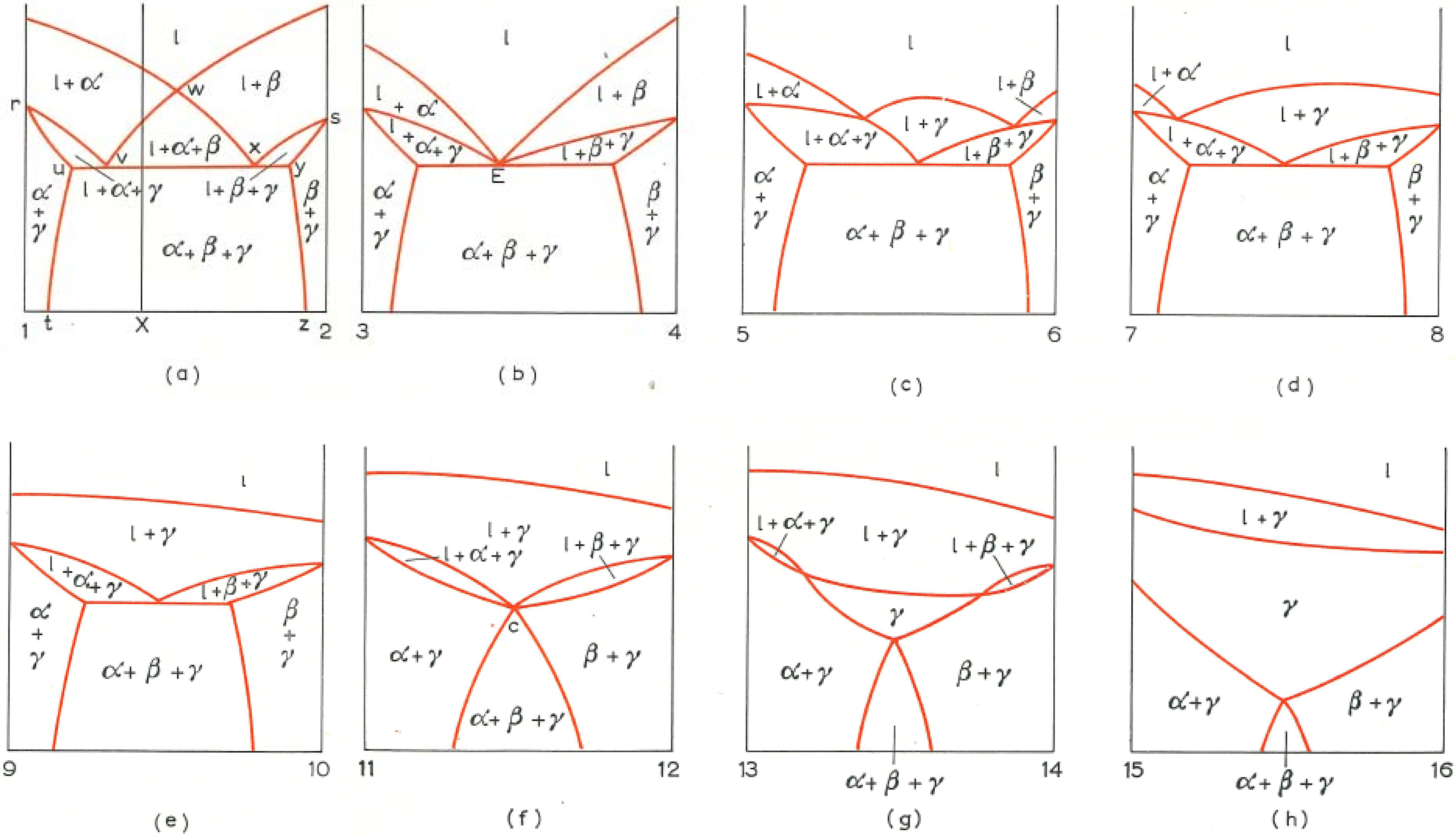

Fig. 178. Vertical sections through the space model of Fig. 173a.

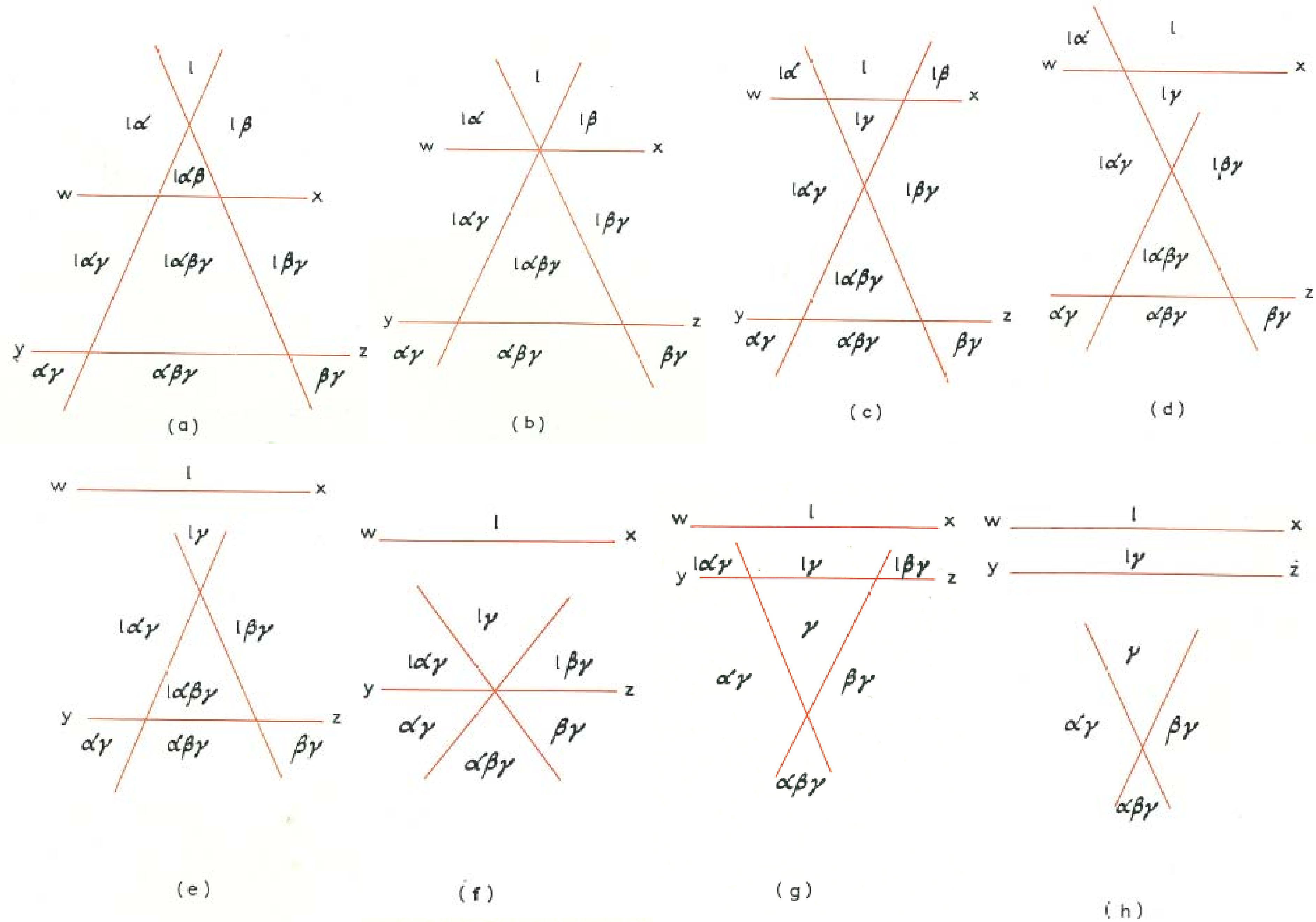

Fig. 245. Formation of the sequence of vertical sections (Fig. 178a–h) by the movement of lines *wx* and *yz*.

14.6. Critical Points

The rule of adjoining phase regions <u>does not apply in the immediate neighborhood of critical points</u> in phase diagrams and their sections.

An empirical formula for the determination of the dimensions of a critical element:

$$R_1 = R - D_c \geqslant 0$$

Where R_1 is the dimension of the boundary between neighboring phase regions,
R is the dimension of the phase diagram or section, and
D_c represents the number of phases that are combined into one phase as a result of the corresponding critical transformation.

Example

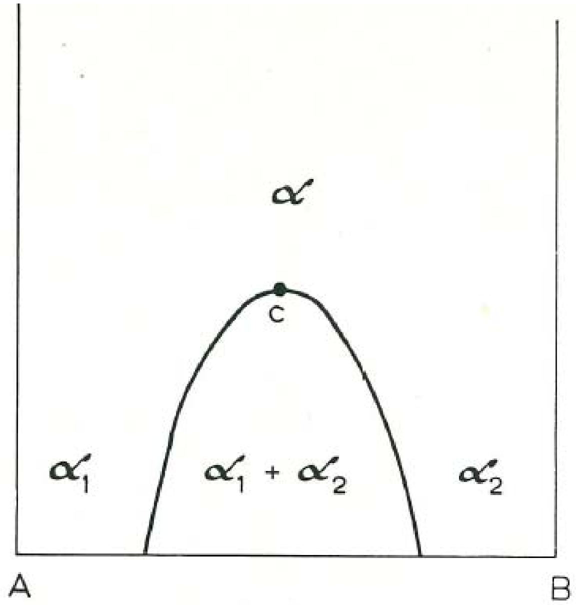

Fig. 246. Binary miscibility gap with critical point c.

$$R_1 = R - D_c = 2 - 2 = 0.$$

The critical element is zero-dimensional—point c.

$$D_c = 2$$

two phases α_1 and α_2 merge at the critical point into the α phase.

Chapter 15. Quaternary phase Diagrams

Four components: A, B, C, D

Assuming isobaric conditions,
Four variables: X_A, X_B, X_C and T

A difficulty of four-dimensional geometry
→ further restriction on the system

Most common figure:
" equilateral tetrahedron "

- 4 pure components
- 6 binary systems
- 4 ternary systems
- A quarternary system

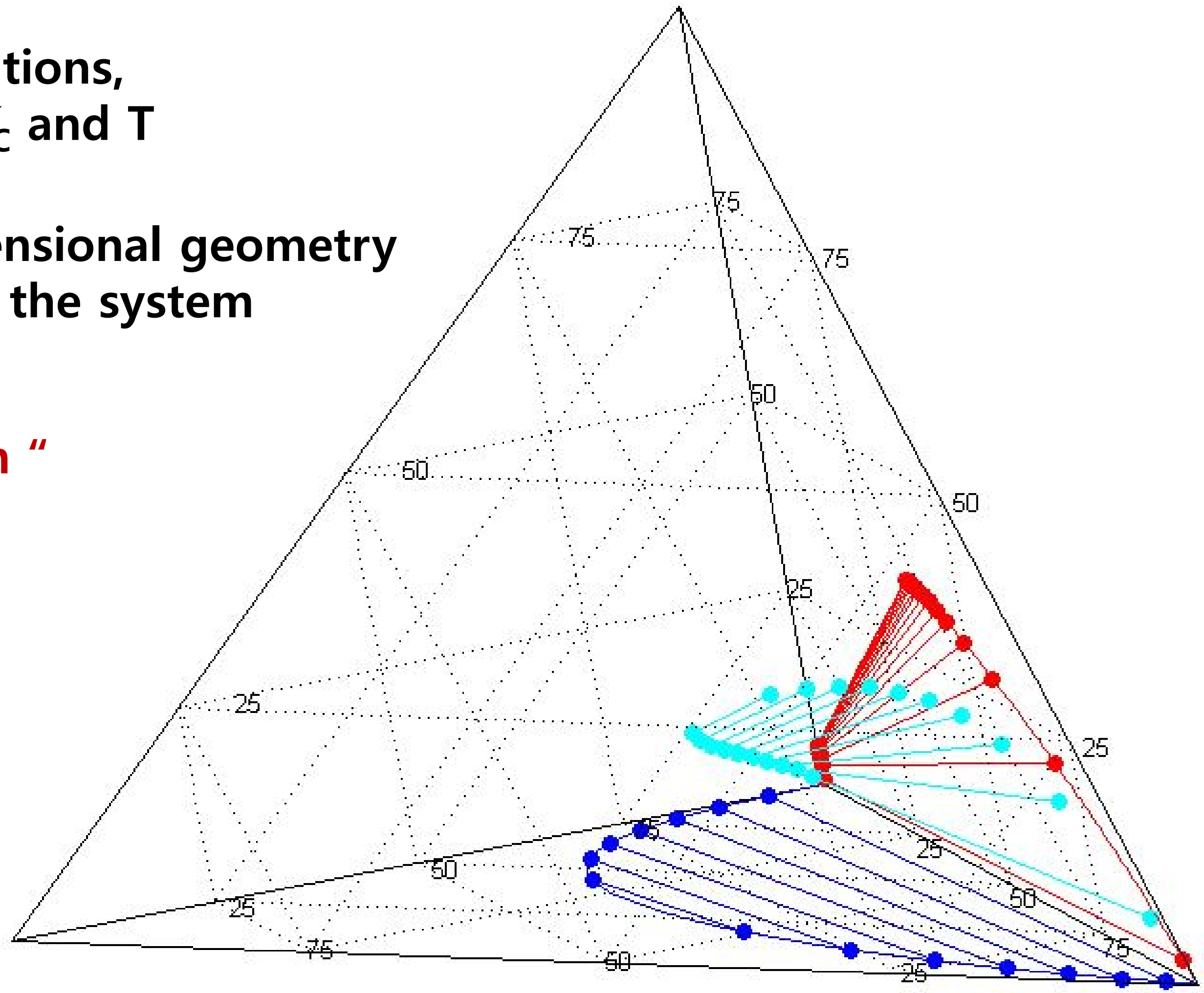

* Draw four small equilateral tetrahedron
→ formed with edge lengths of a, b, c, d

$$a+b+c+d=100$$

%A=Pt=c,
%B=Pr=a,
%C=Pu=d,
%D=Ps=b

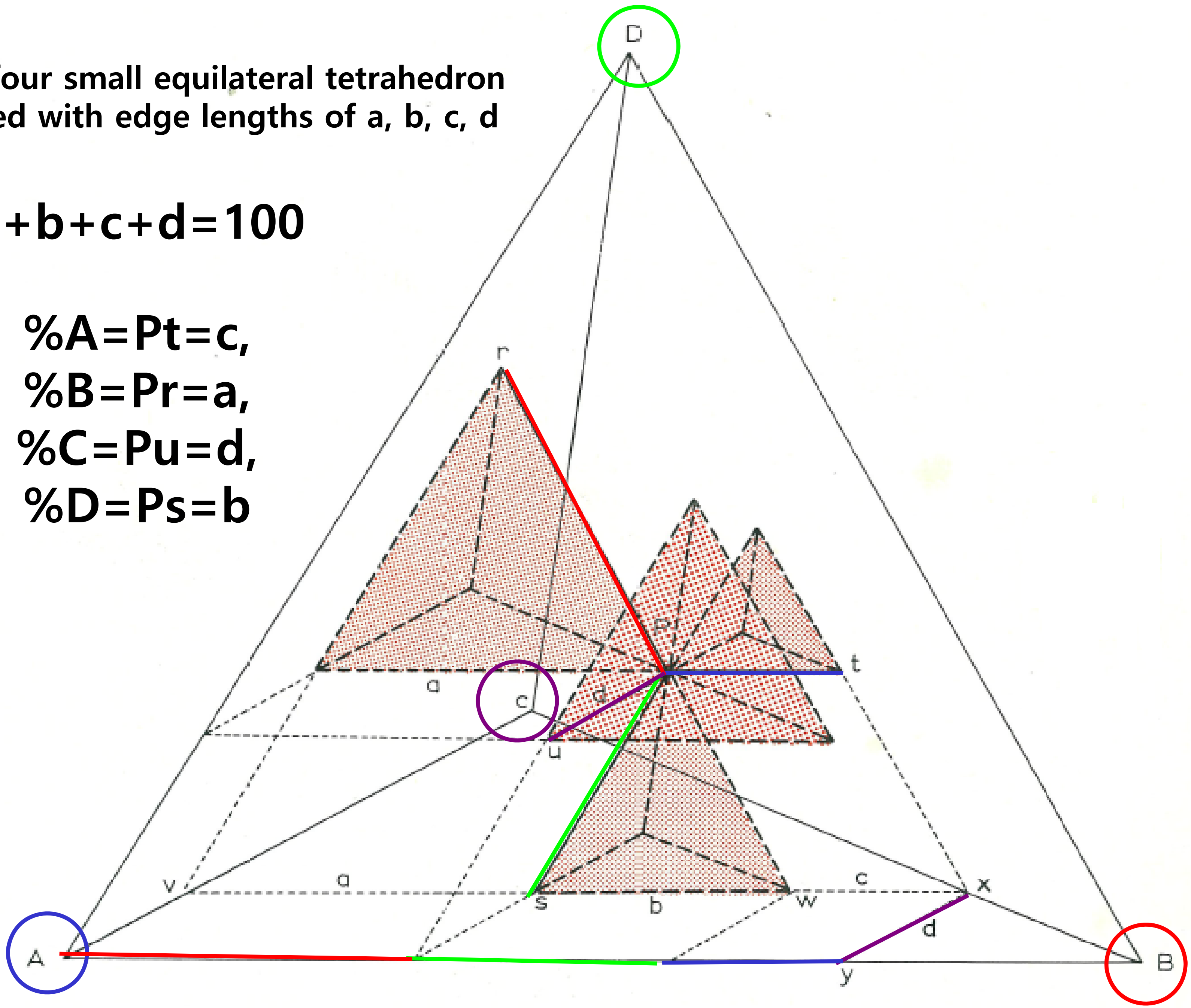

Fig. 247. Representation of a quaternary system by an equilateral tetrahedron.

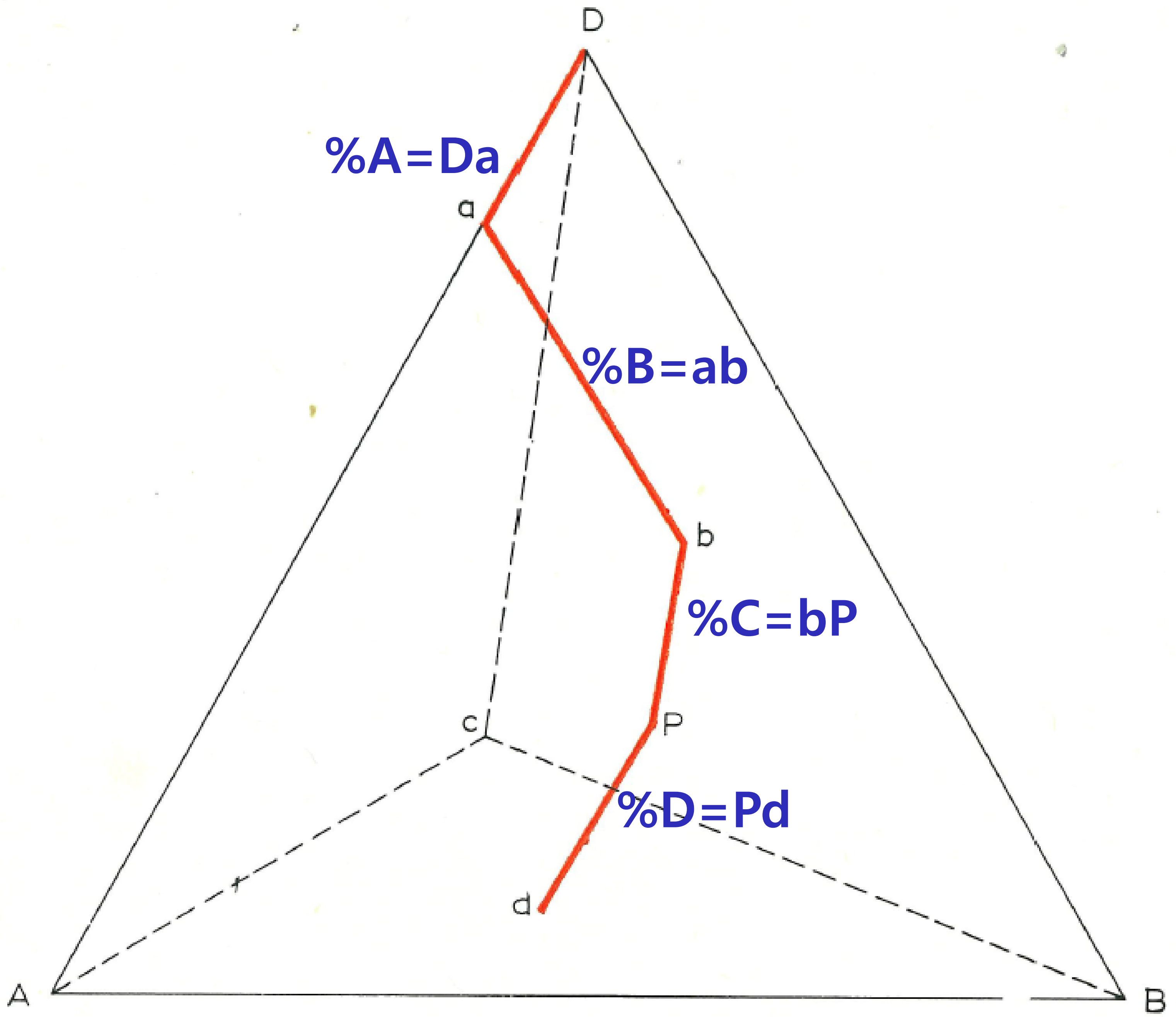

Fig. 248. Plotting of alloy compositions in quaternary systems.

Useful geometrical properties of an equilateral tetrahedron

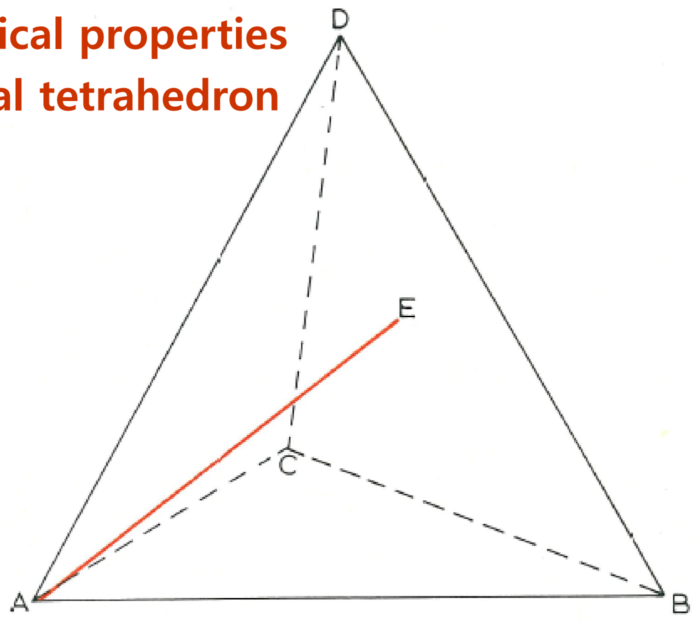

B:C:D constant on line *AE*

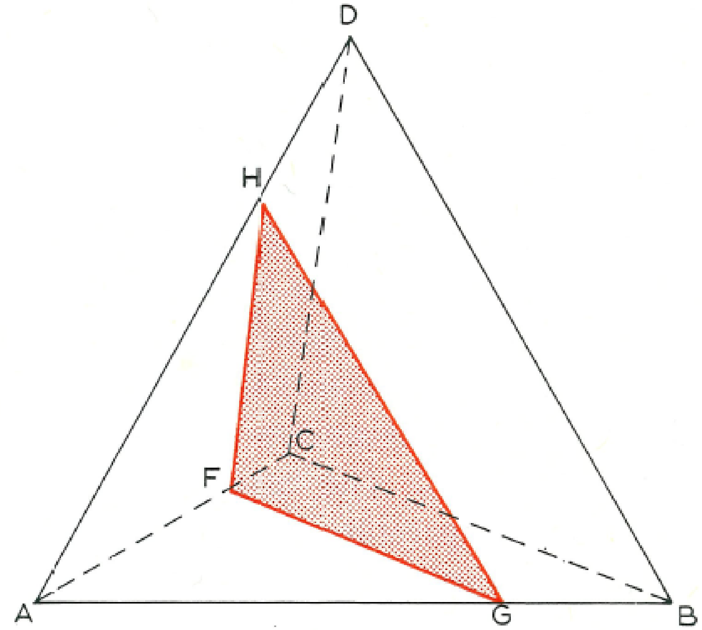

A constant on plane *FGH*

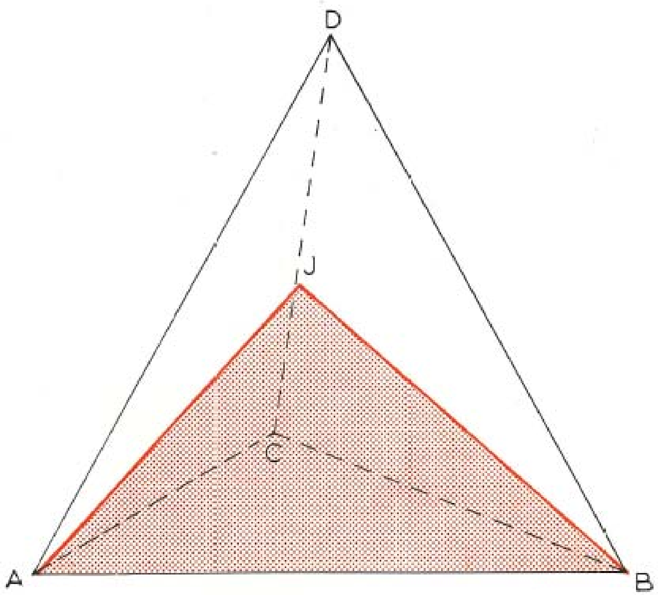

C:D constant on plane *ABJ*

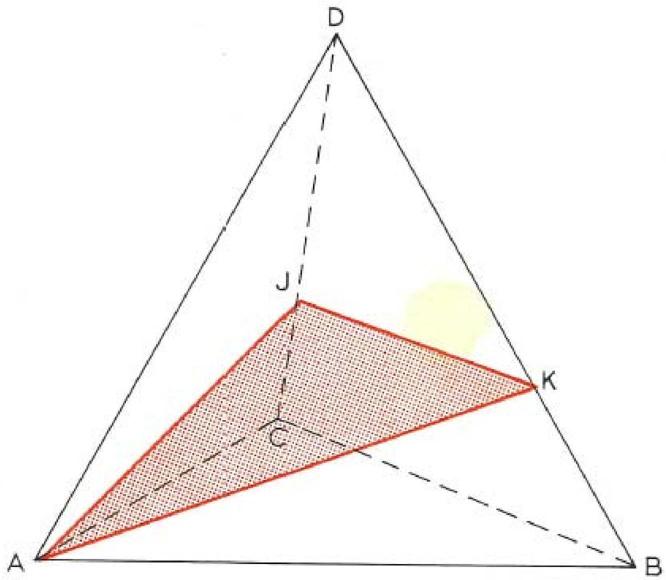

C:D and B:D constant on plane *AJK*

The three-dimensional equilateral tetrahedron can be used to study quaternary equilibria in the following ways.

1) Isobaric-isothermal sections (both P and T are fixed)

It is necessary to produce a series of three-dimensional tetrahedra to indicate the equilibria at a series of temperatures.

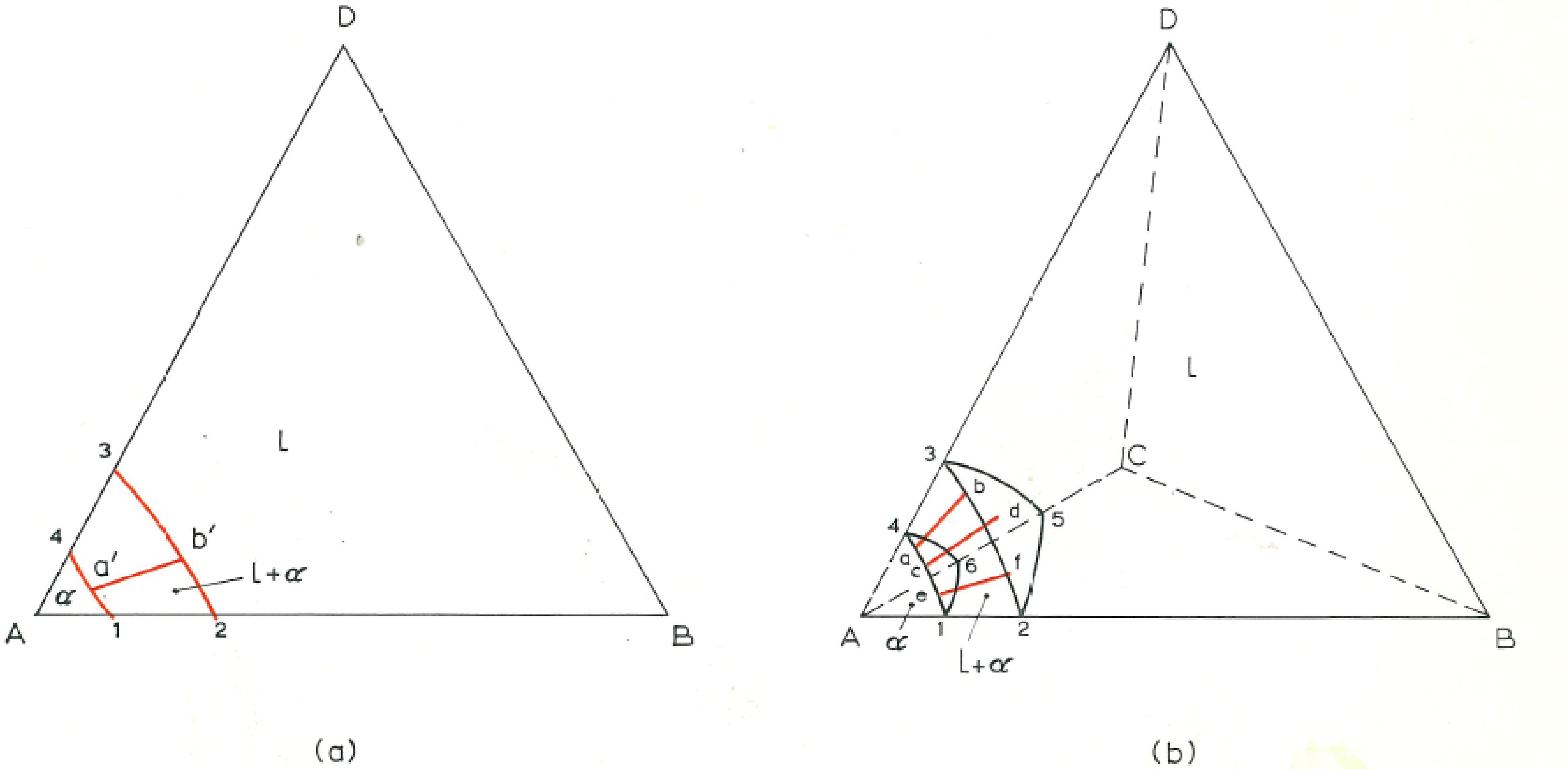

Fig. 251. Isobaric–isothermal sections for systems involving two-phase equilibrium. (a) Ternary system; (b) quaternary system.

10.1. THE EUTECTIC EQUILIBRIUM ($l = \alpha + \beta + \gamma$)

- **Isothermal section** ($T_A > T > T_B$)

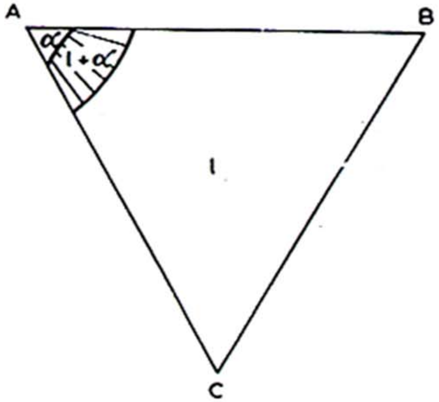

(a) $T_A > T > T_B$

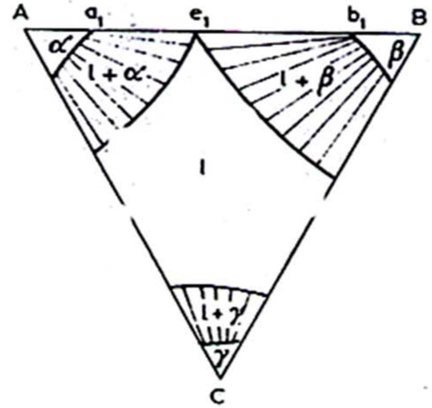

(b) $T = e_1$

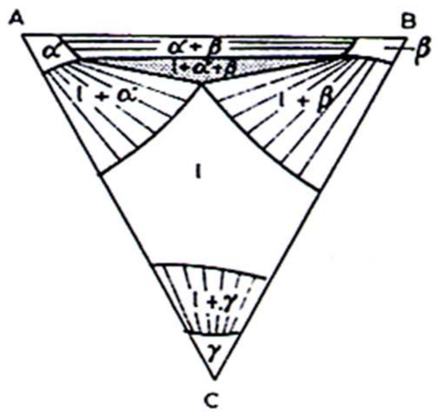

(c) $e_1 > T > e_3$

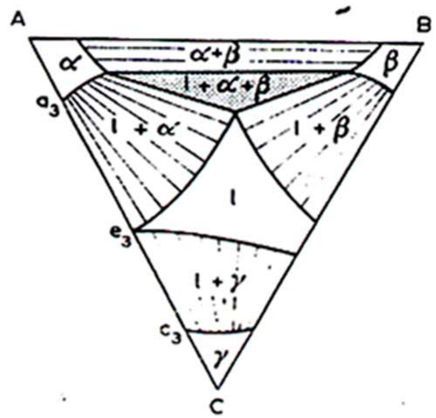

(d) $T = e_3$

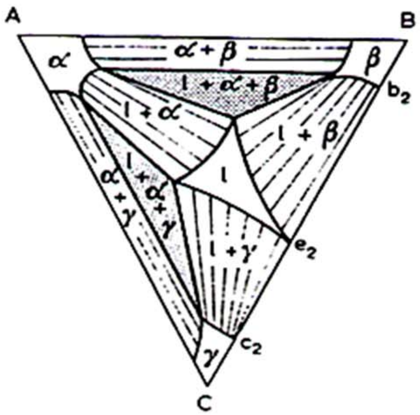

(e) $T = e_2$

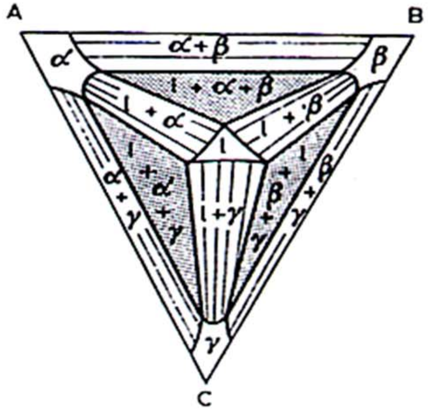

(f) $e_2 > T > E$

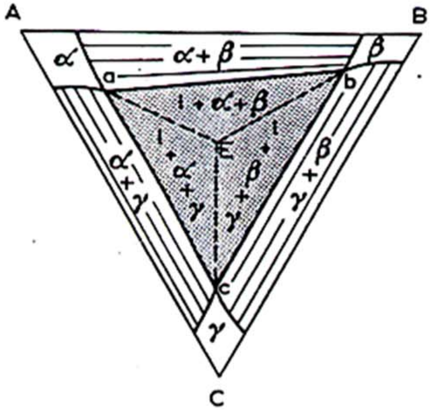

(g) $T_A = E$

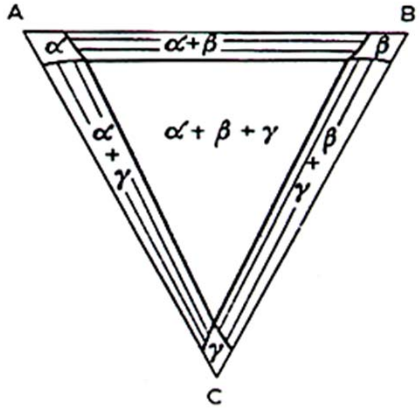

(h) $E = T$

2) Polythermal sections

10.1. THE EUTECTIC EQUILIBRIUM ($l = \alpha + \beta + \gamma$)

<u>Ternary eutectic</u> • Projection : solid solubility limit surface

: monovariant liquidus curve

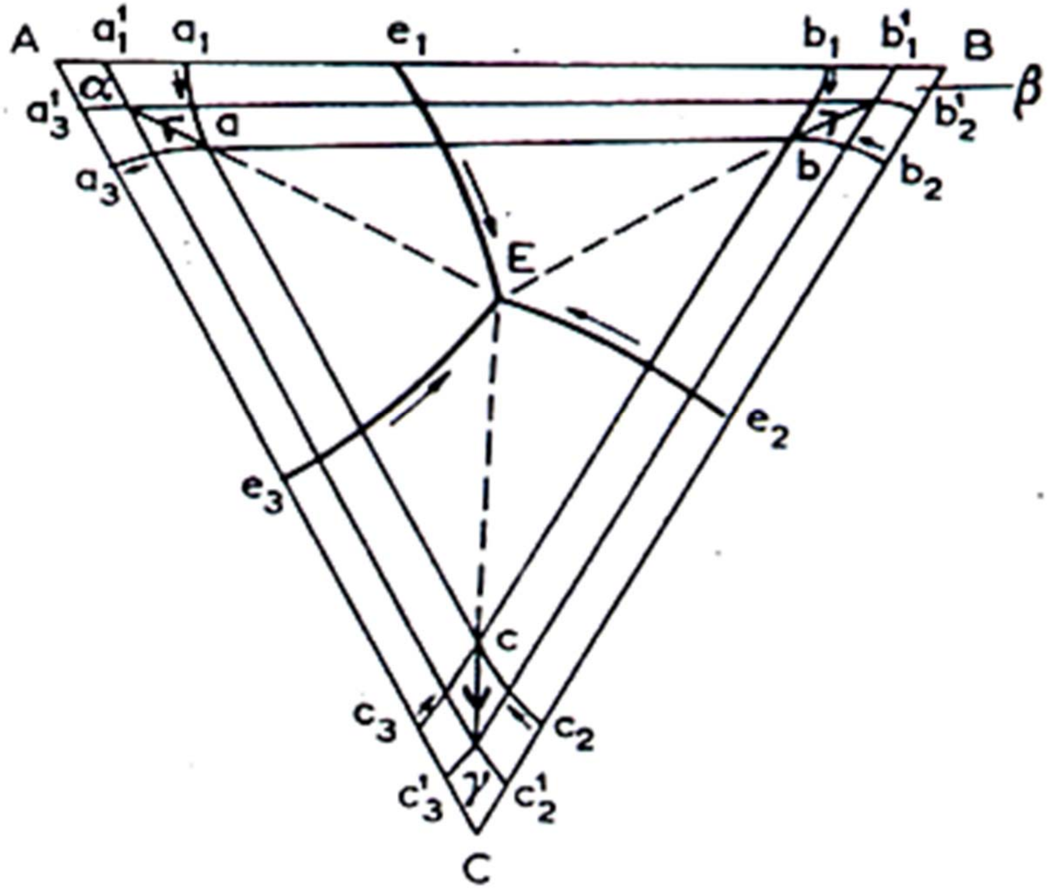

2) Polythermal sections

(1) Quaternary system: a polythermal projection which is three dimensional

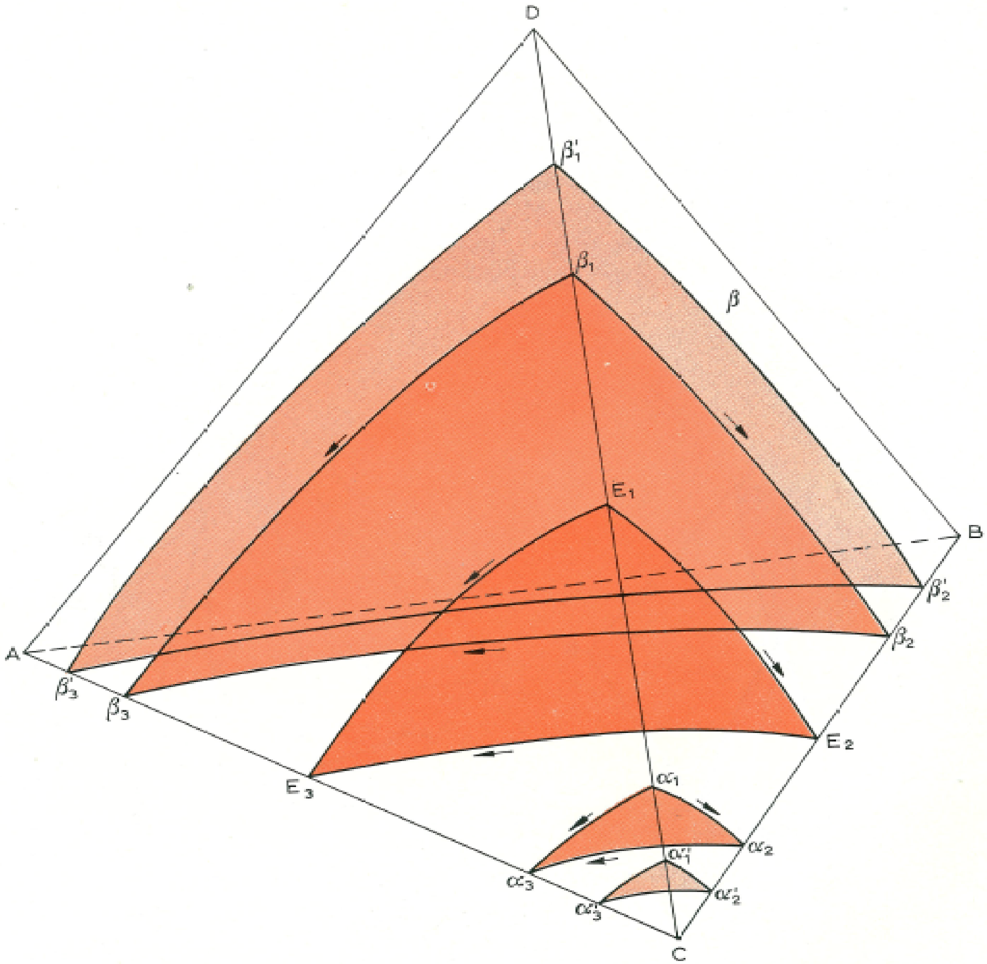

Fig. 255. Polythermal projection of a quaternary system involving three-phase equilibrium of the type l $\rightleftarrows \alpha + \beta$

2) Polythermal sections

(2) Temperature-concentration sections: either 3-dimensional or 2-dimensional

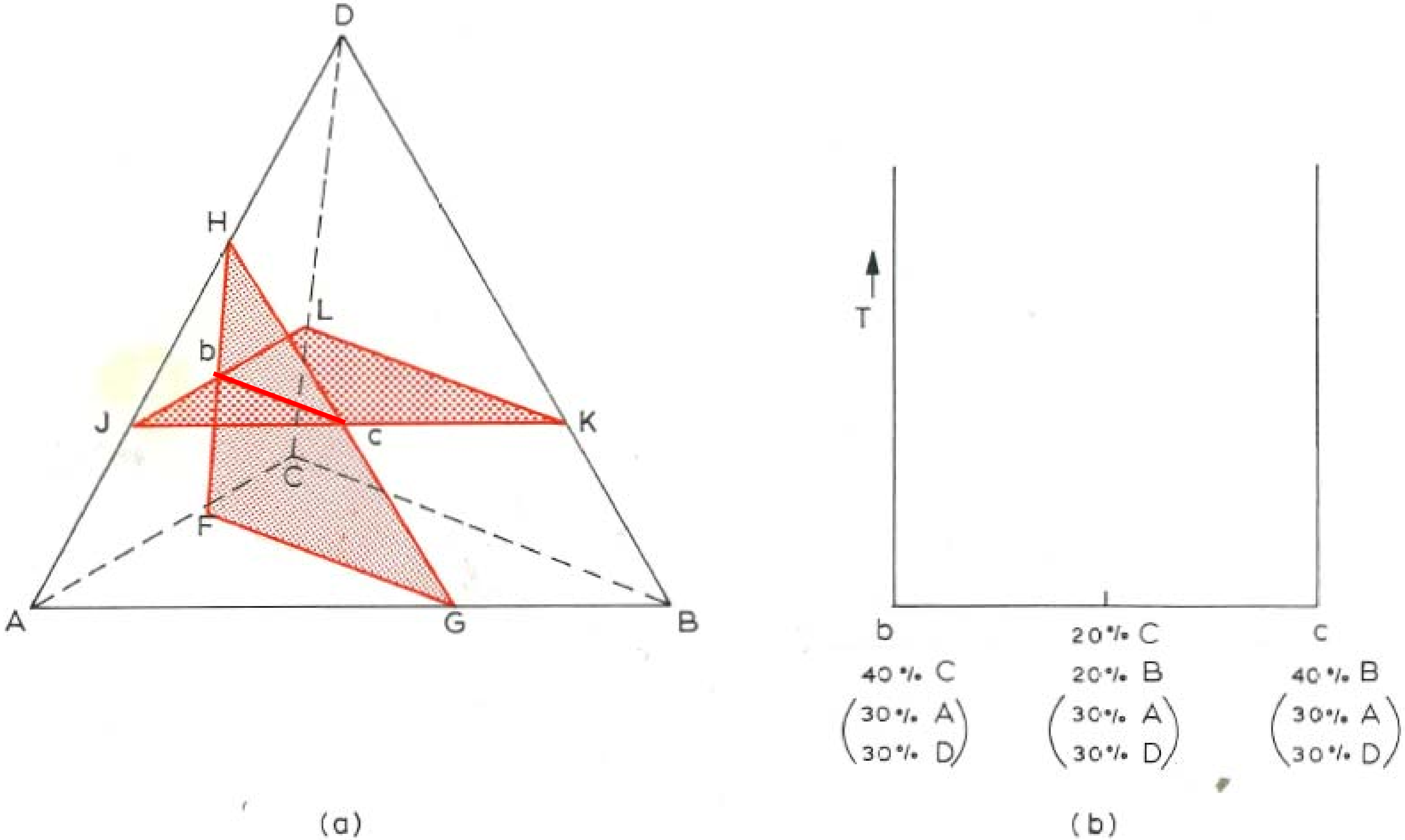

Fig. 250. Production of a two-dimensional section through a quaternary system. (a) Alloys on line *bc* contain constant content of A and D; (b) erection of temperature axis on line *bc* to give the two-dimensional section.

15.2 TWO-PHASE EQUILIBRIUM

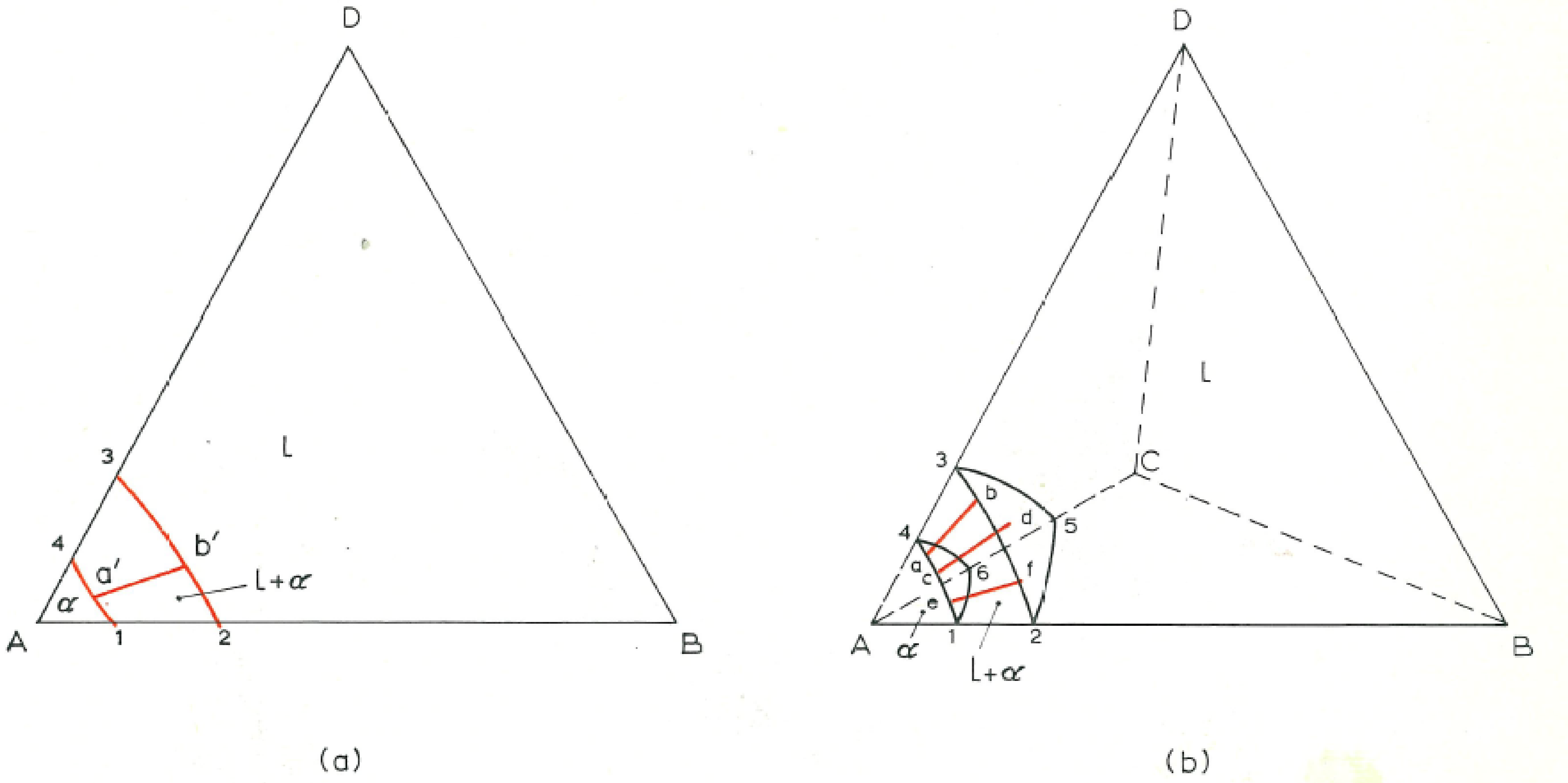

Fig. 251. Isobaric–isothermal sections for systems involving two-phase equilibrium. (a) Ternary system; (b) quaternary system.

Tie lines in (b) connect all points of surface 3 5 2 to corresponding points on surface 4 6 1. → <u>They do not intersect one another</u>.

*** Isobaric-isothermal sections through a quaternary system involving two-phase equilibrium**

$T_B > T_A > T_D > T_C$

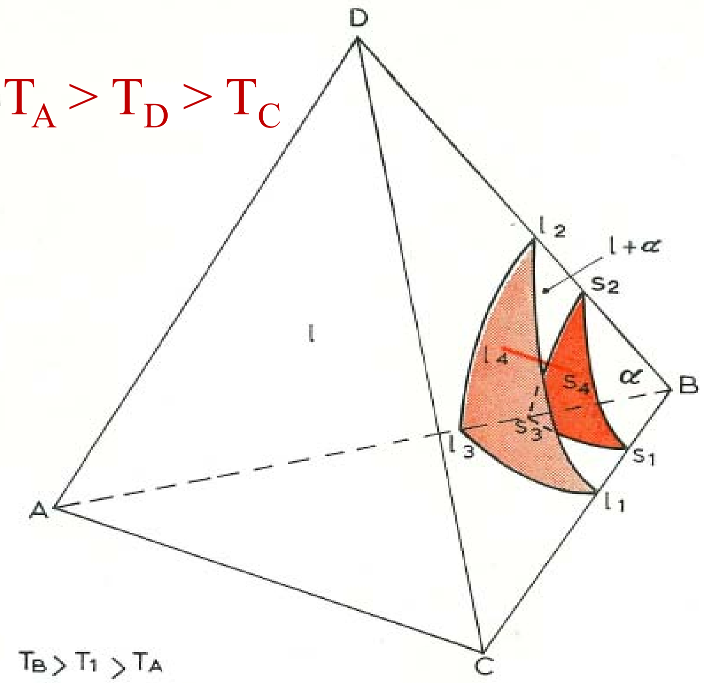

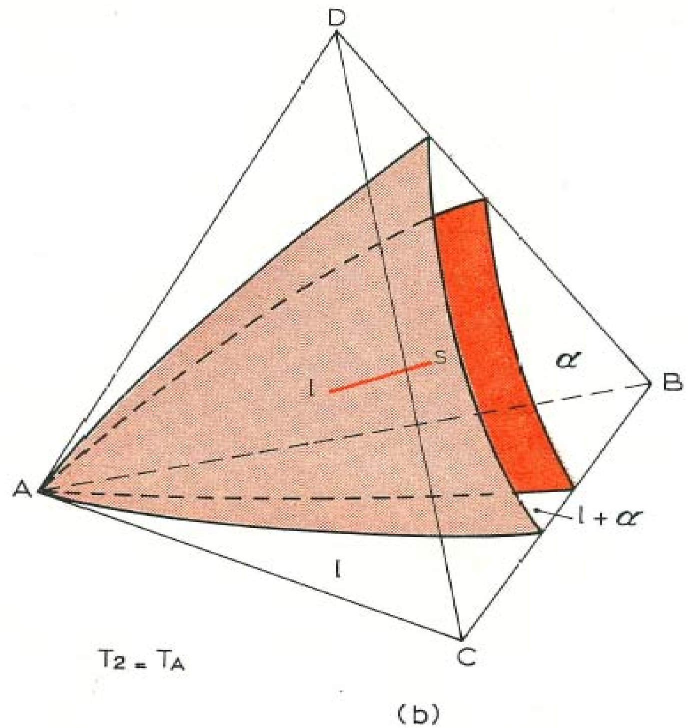

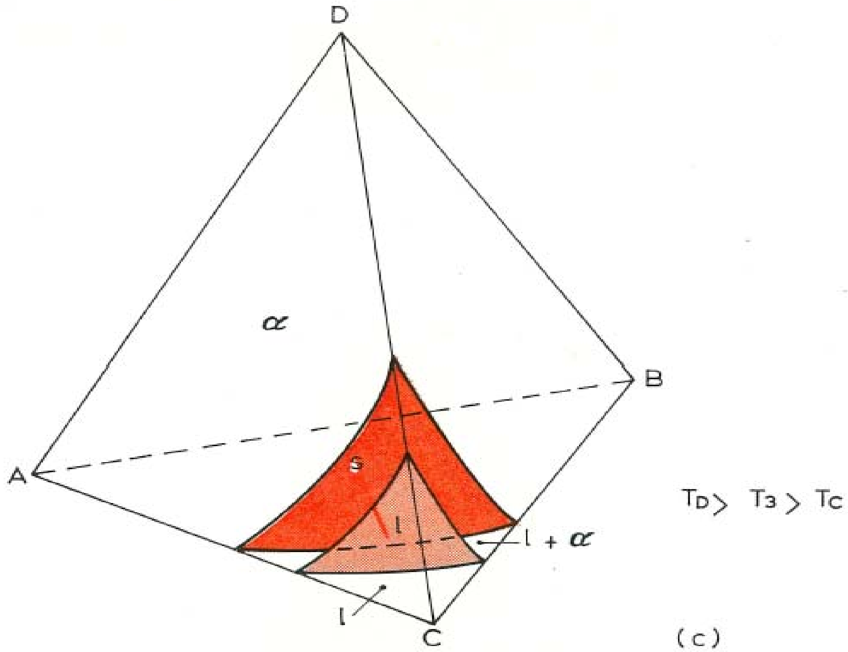

* <u>The quaternary tie lines</u> are going from one isothermal section to another with decreasing temperature the tie lines <u>all change their orientation</u>.

* <u>The quaternary melt is richer in the lower-melting components than the quaternary solid solution</u> it is in equilibrium with <u>Konovalov's rule</u>.

* The usual lever rule is applicable to tie lines in quaternary systems.

This rotation coincides with the direction of highest melting point component to the lowest.

Konovalov's Rule: Solid is always richer than the melt with which it is in equilibrium in that component which raises the melting point when added to the system.

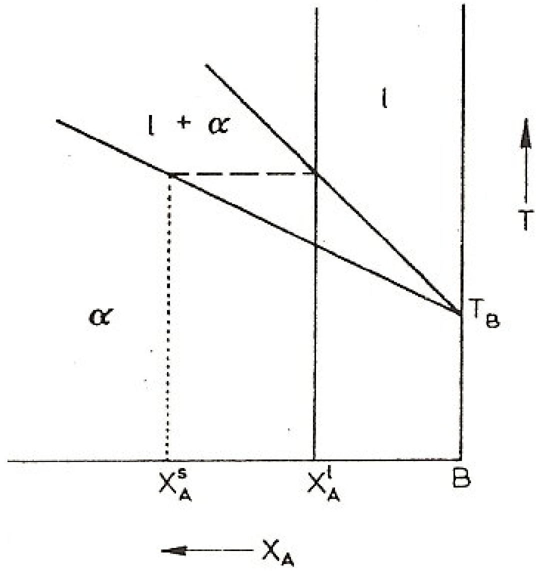

$$X_A^S > X_A^l$$

$$X_A^S + X_B^S = X_A^l + X_B^l = 1$$

then

$$\frac{X_A^S}{X_A^S + X_B^S} > \frac{X_A^l}{X_A^l + X_B^l}$$

$$X_A^S > X_A^l$$

and

$$\frac{X_A^S}{X_A^S + X_B^S - X_A^S} > \frac{X_A^l}{X_A^l + X_B^l - X_A^l}$$

Therefore,

$$\frac{X_A^S}{X_B^S} > \frac{X_A^l}{X_B^l}$$

In this form Konovalov's Rule can be applied to ternary systems to indicate the direction of tie lines.

8.4 TWO-PHASE EQUILIBRIUM

8.4.1 Two-phase equilibrium between the liquid and a solid solution

(iv) Tie lines at T's will rotate continuously. (Konovalov's Rule)

: Clockwise or counterclockwise

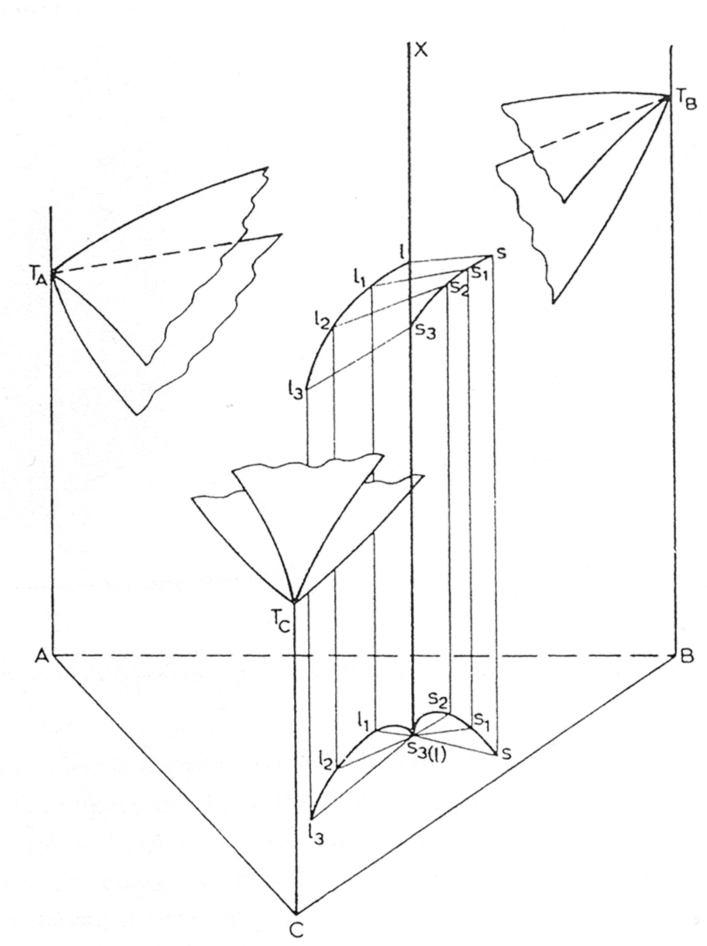

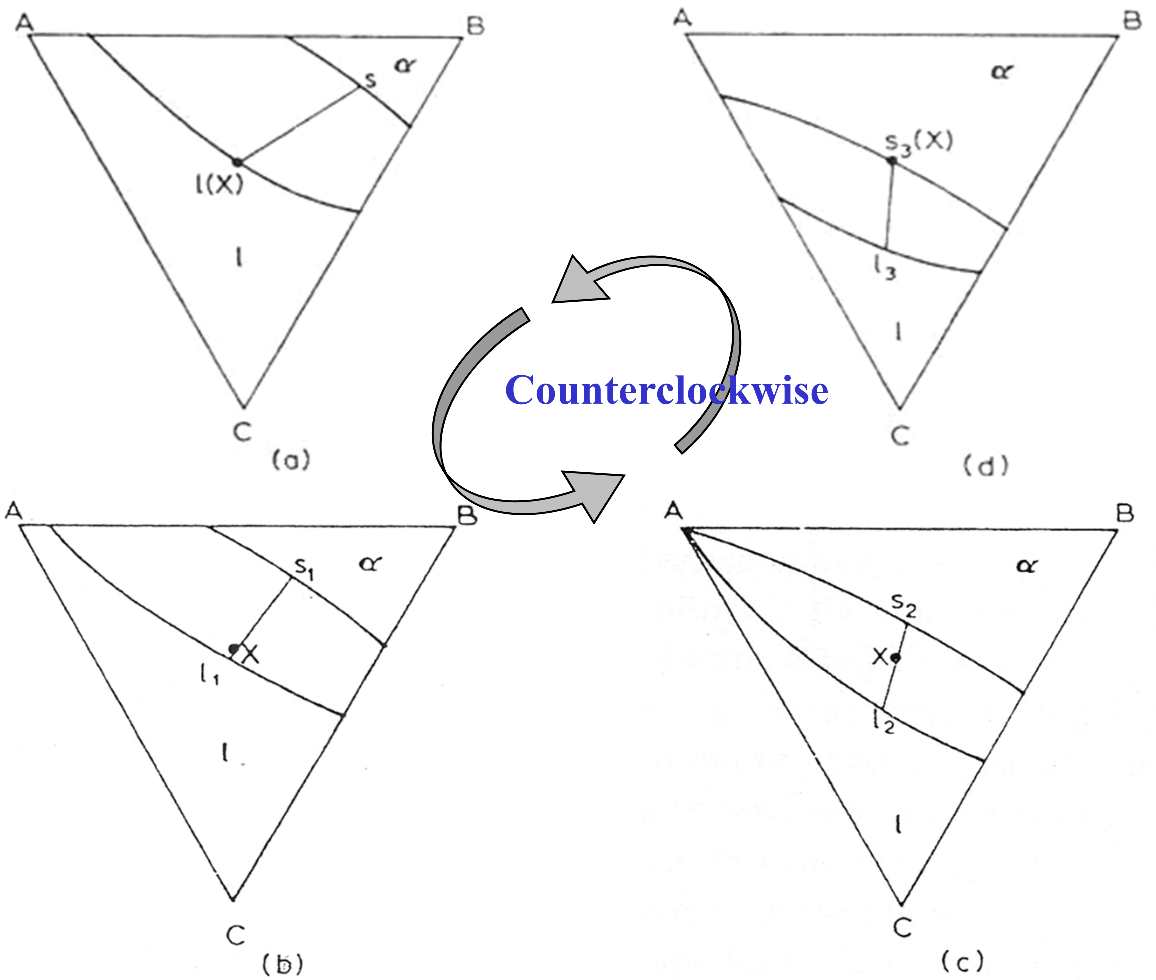

* Course of solidification of quaternary alloy P

* T_1 : liquidus surface $m_1m_2m_3 \rightarrow P$
  Solidus surface $s_1s_2s_3 \rightarrow \alpha_1$

* T_2 : tie line $\alpha_2 l_2$
  → this tie line is not parallel to the first tie line $P\alpha_1$ in contrast to the series of tie lines in the ternary system.

* T_3 : liquidus surface $m_7m_8A \rightarrow l_3$
  Solidus surface $s_7s_8A \rightarrow P$

* Liquid trace curve: Pl_2l_3
  α phase trace curve: $\alpha_1\alpha_2P$

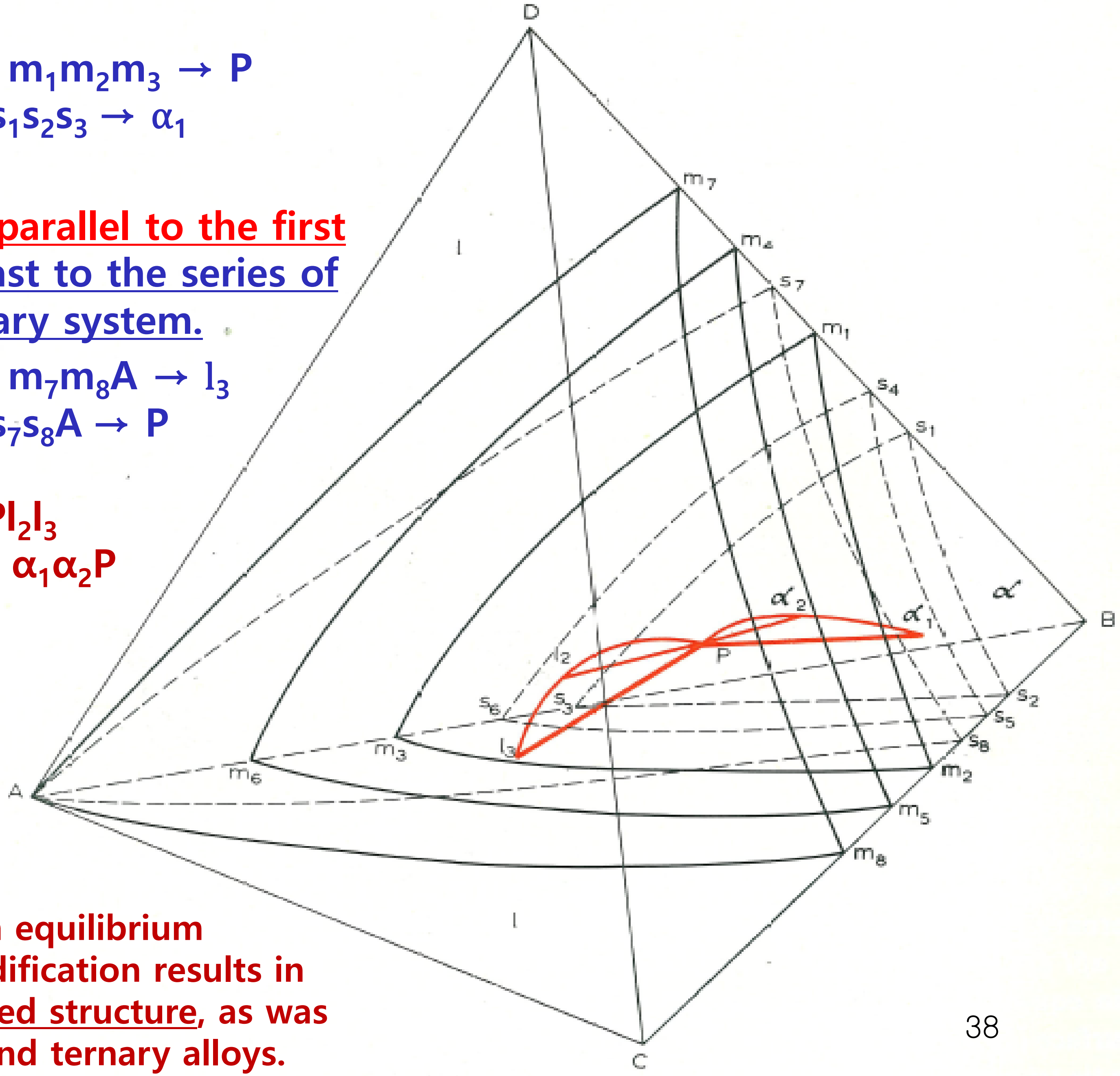

→ Any departure from equilibrium conditions during solidification results in the formation of a cored structure, as was noted for the binary and ternary alloys.

15.3 THREE-PHASE EQUILIBRIUM

* The tie triangles in the quaternary three-phase region do not lie parallel to each other, in contrast to the superficially similar three-phase region in a ternary (isobaric) space model.

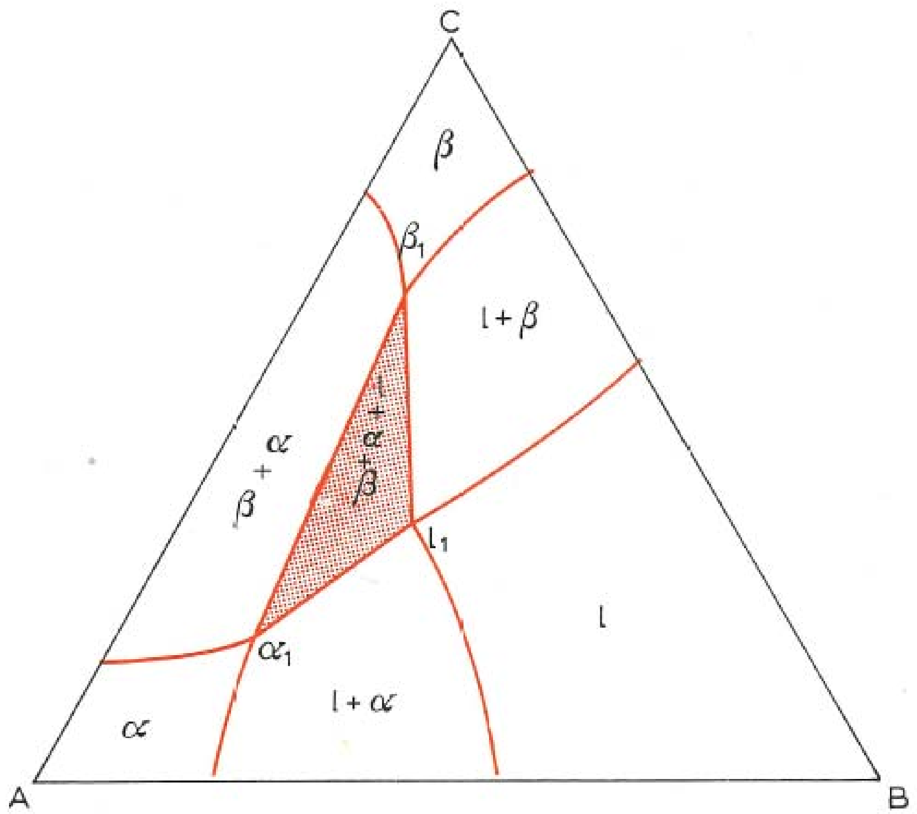

(a) Ternary system

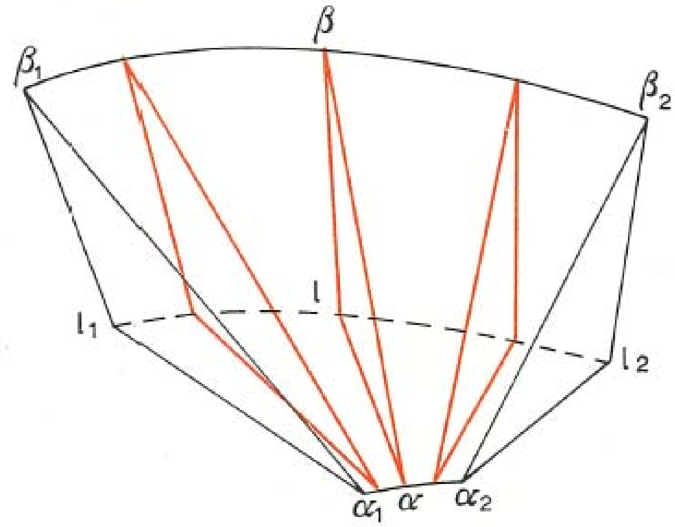

(b) quaternary system

Fig. 254. Isobaric-isothermal sections for systems involving three-phase equilibrium.

Fig. 255. Polythermal projection of a quaternary system involving three-phase equilibrium of the type $l \rightleftarrows \alpha + \beta$

$T_D > T_C > E_1 > T_B > T_A > E_2 > E_3$

* Binary eutectic: CA, CB, CD
& A, B, D form continuous series of binary solid solution with each other.

* Face *ACD* of the tetrahedron ABCD= polythermal projection of the ternary system ACD

: Continuous transition from the binary eutectic CD to the binary eutectic AC (monovariant liquidus curve E_1E_3)

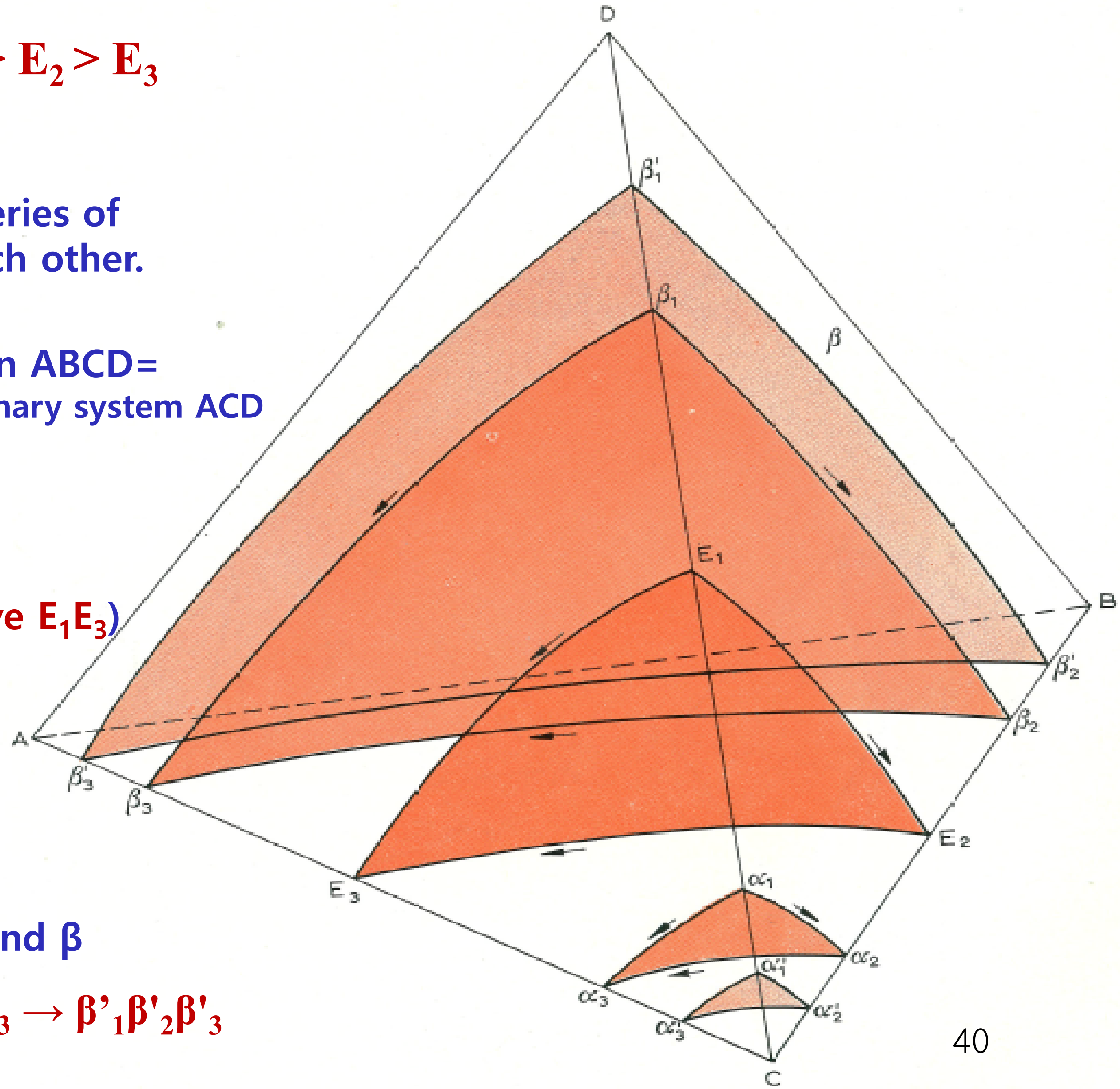

* Change in solubility in α and β

$\alpha_1\alpha_2\alpha_3 \rightarrow \alpha'_1\alpha'_2\alpha'_3$, $\beta_1\beta_2\beta_3 \rightarrow \beta'_1\beta'_2\beta'_3$

$T_D > T_C > E_1 > T_B > T_A > E_2 > E_3$

Fig. 256. Isobaric-isothermal sections through the quaternary system of Fig. 255

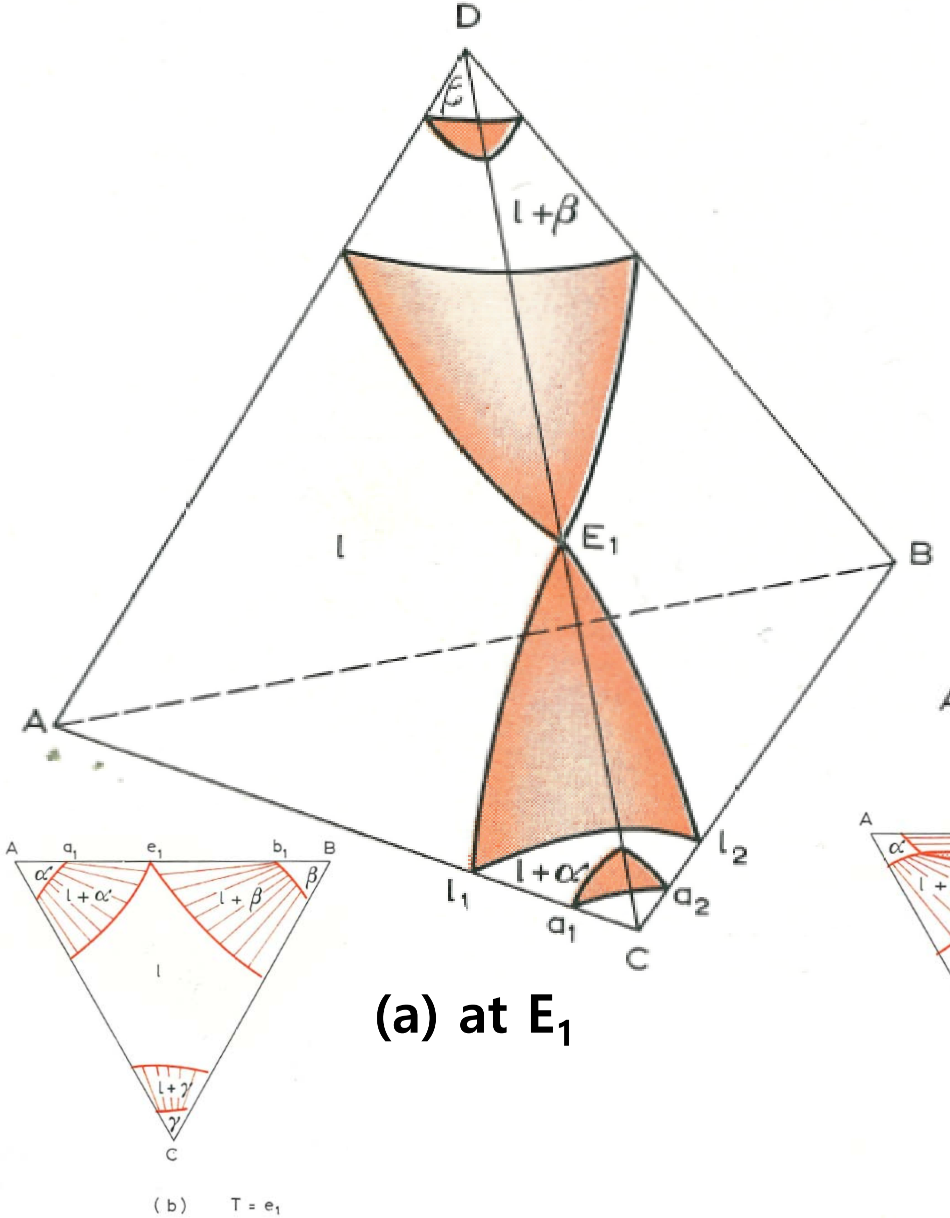

(a) at E_1

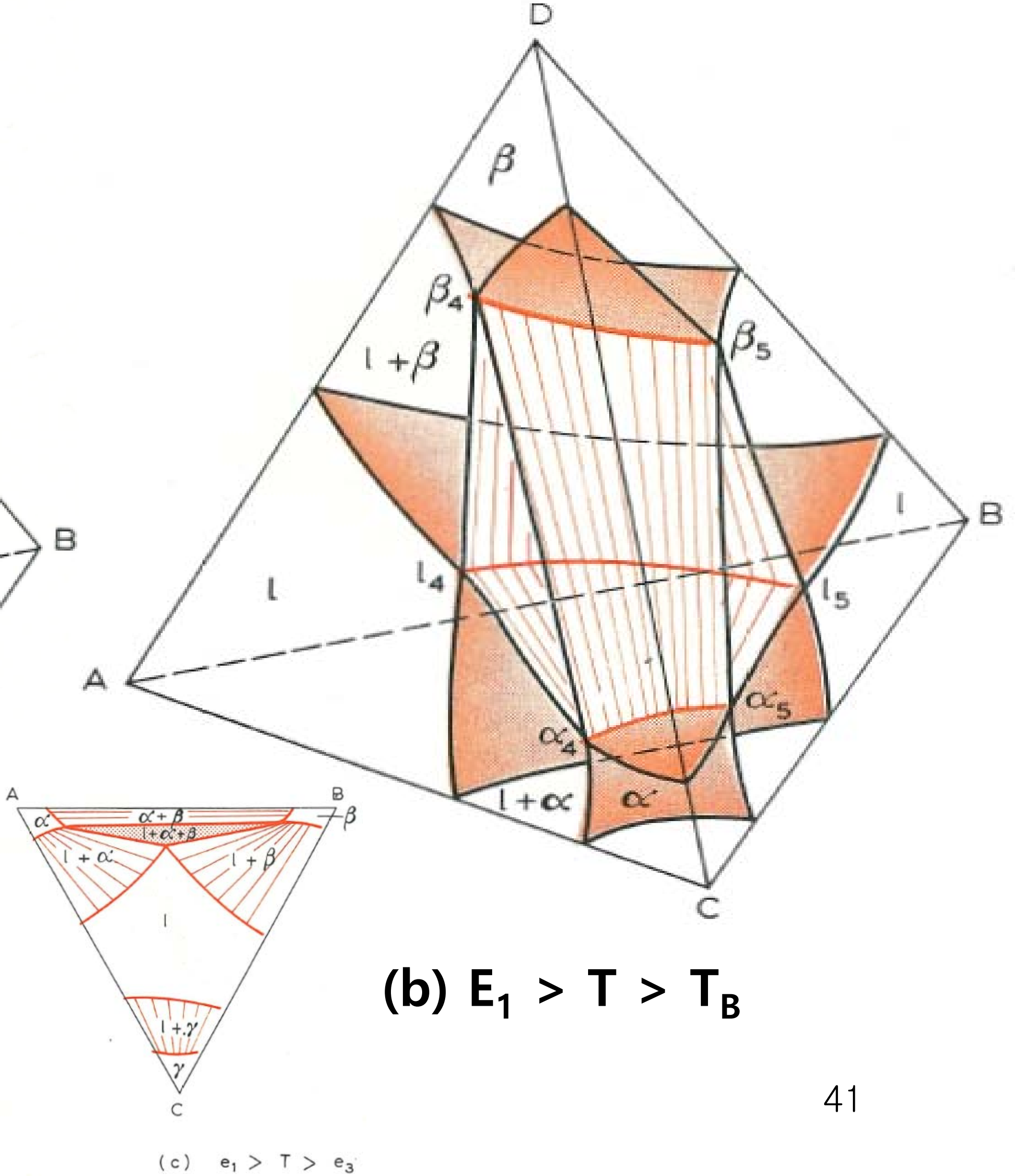

(b) $E_1 > T > T_B$

$T_D > T_C > E_1 > T_B > T_A > E_2 > E_3$

Fig. 256. Isobaric-isothermal sections through the quaternary system of Fig. 255

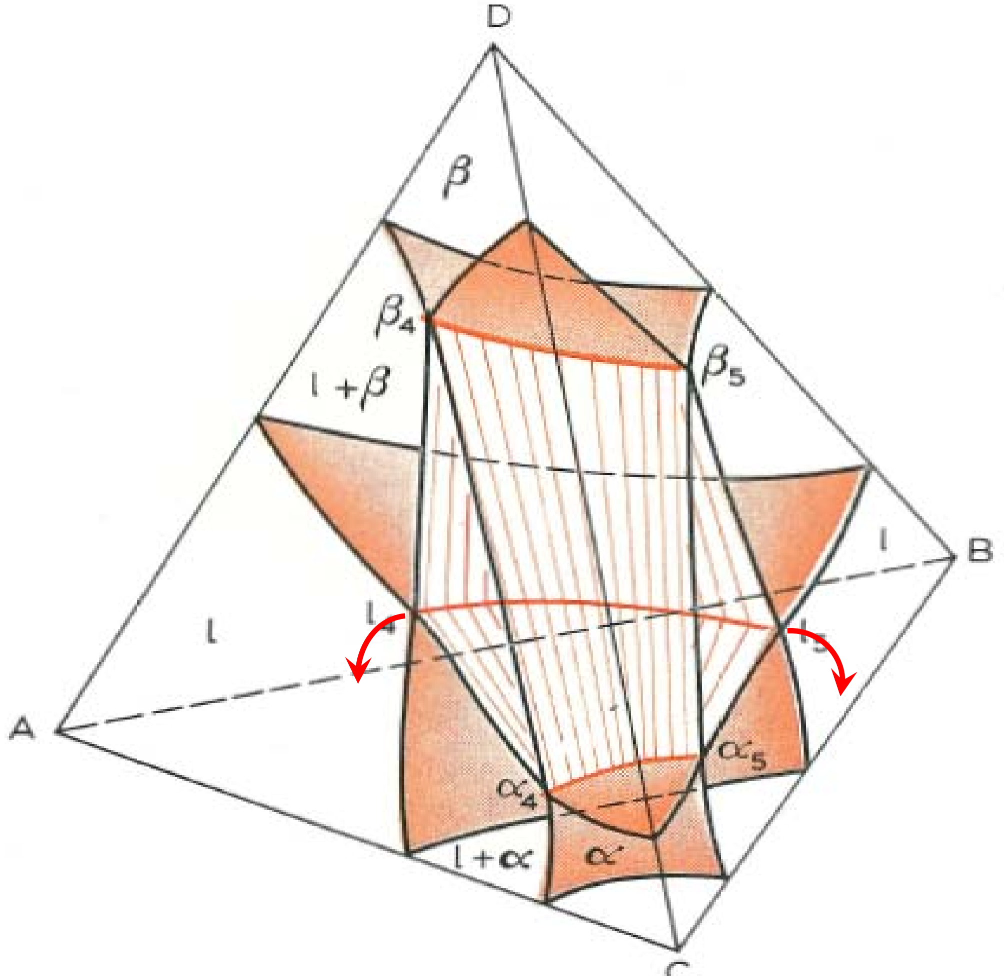

(b) E_1 > T > T_B

*** Quaternary three phase region**

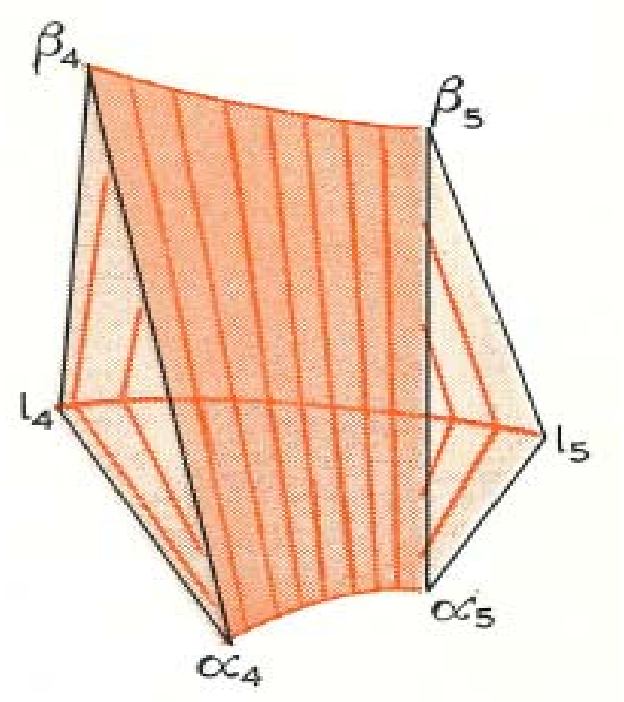

$T_D > T_C > E_1 > T_B > T_A > E_2 > E_3$

Fig. 256. Isobaric-isothermal sections through the quaternary system of Fig. 255

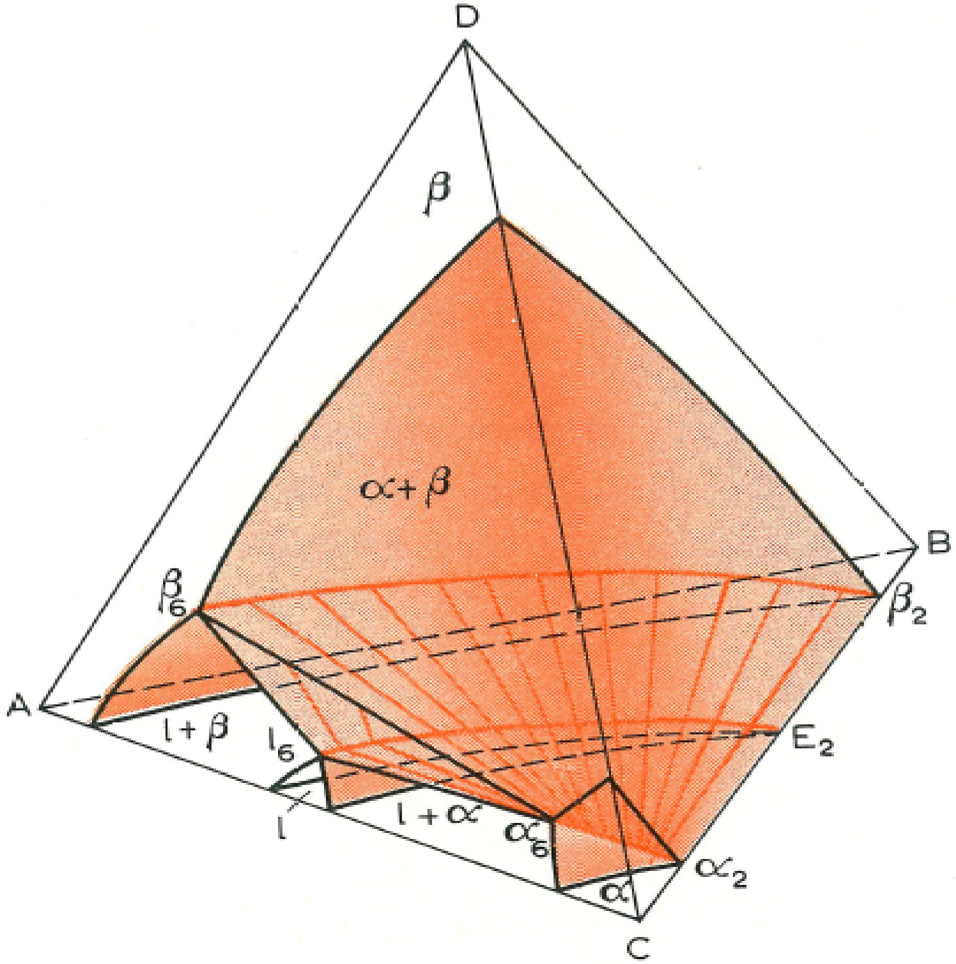

(d) at E_2

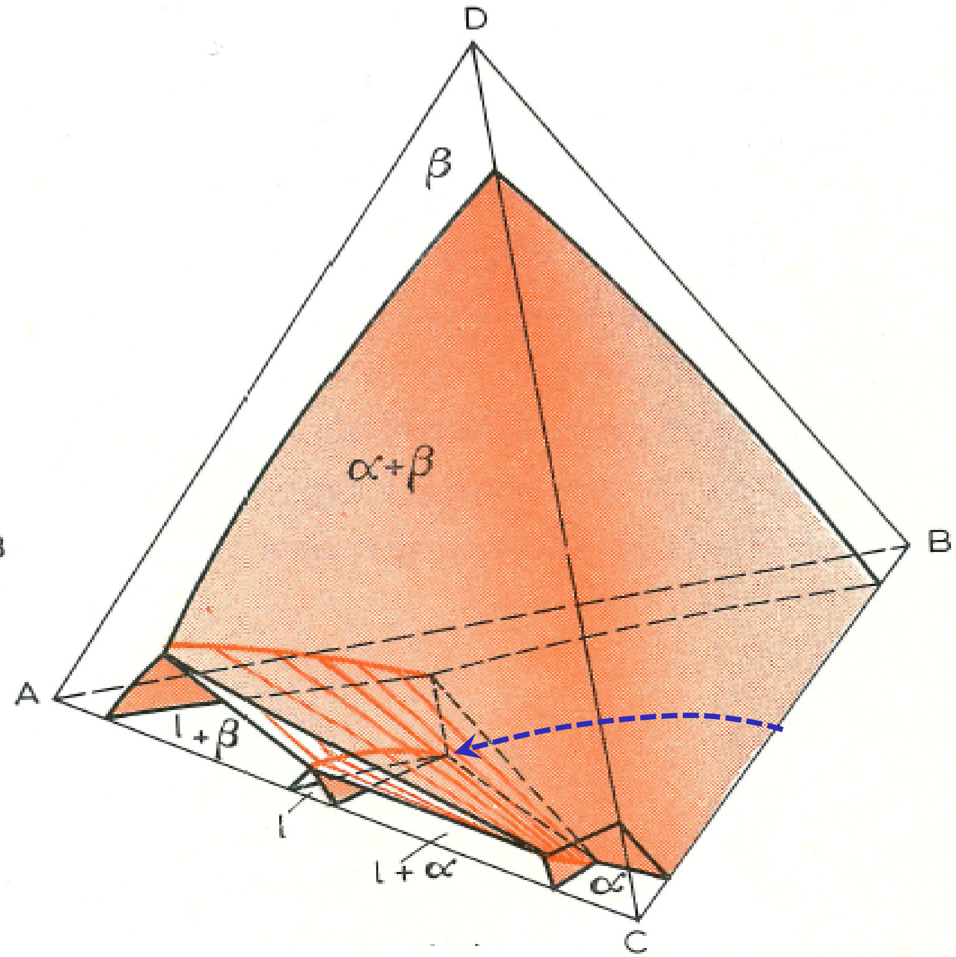

(e) E_2 > T > E_3

$T_D > T_C > E_1 > T_B > T_A > E_2 > E_3$

Fig. 256. Isobaric-isothermal sections through the quaternary system of Fig. 255

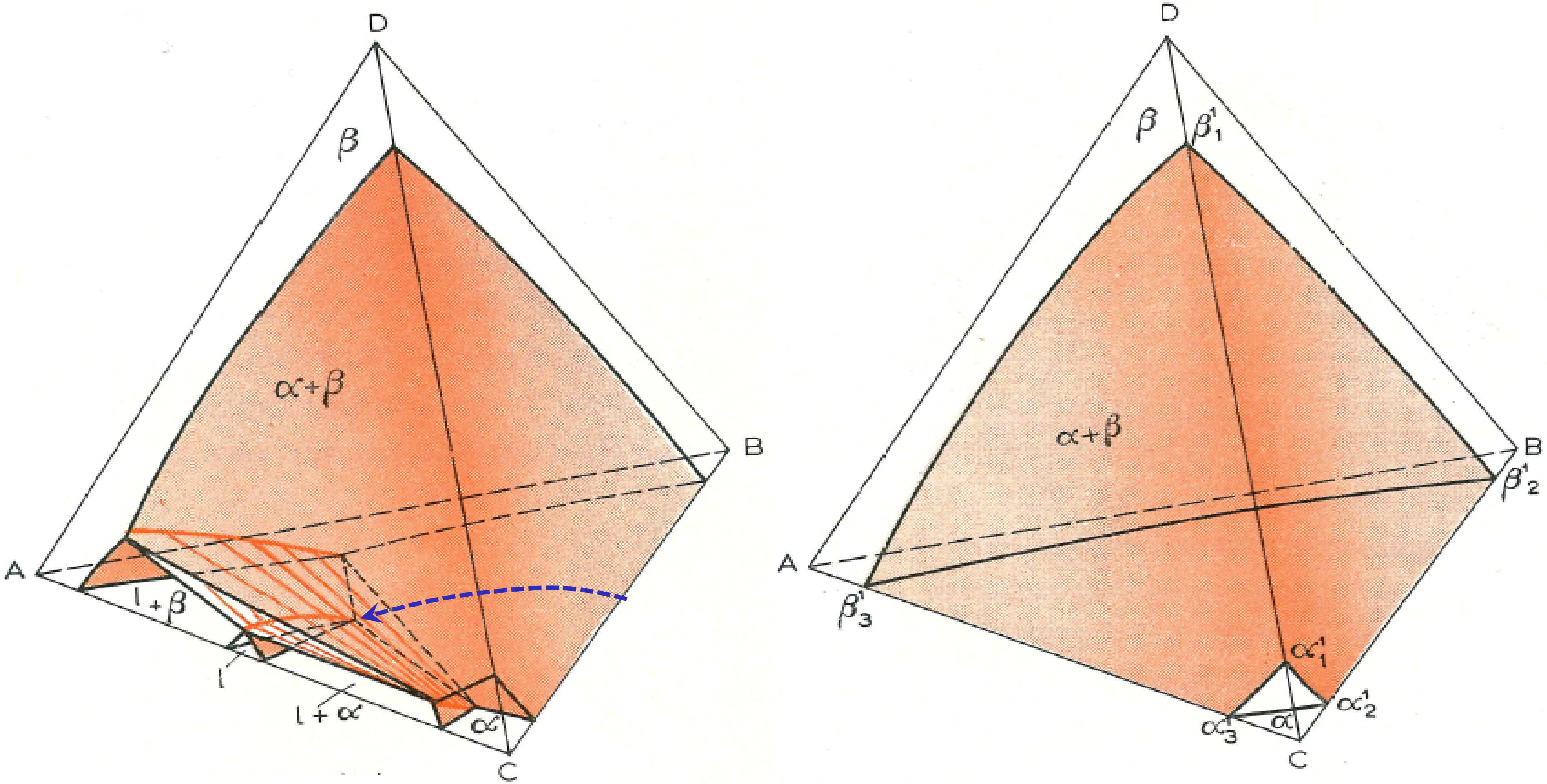

(e) E_2 > T > E_3 **(f) below E_3**

1) At E_3, the last drop of liquid is consumed and all alloys in the quaternary system are completely solid at temperatures below E_3.

2) Below E_3, change in solubility in α and β ($\alpha_1\alpha_2\alpha_3 \rightarrow \alpha'_1\alpha'_2\alpha'_3$, $\beta_1\beta_2\beta_3 \rightarrow \beta'_1\beta'_2\beta'_3$)

The three-phase regions from Fig. 256.b, d, and e have been superimposed on the polythermal projection in Fig. 257.

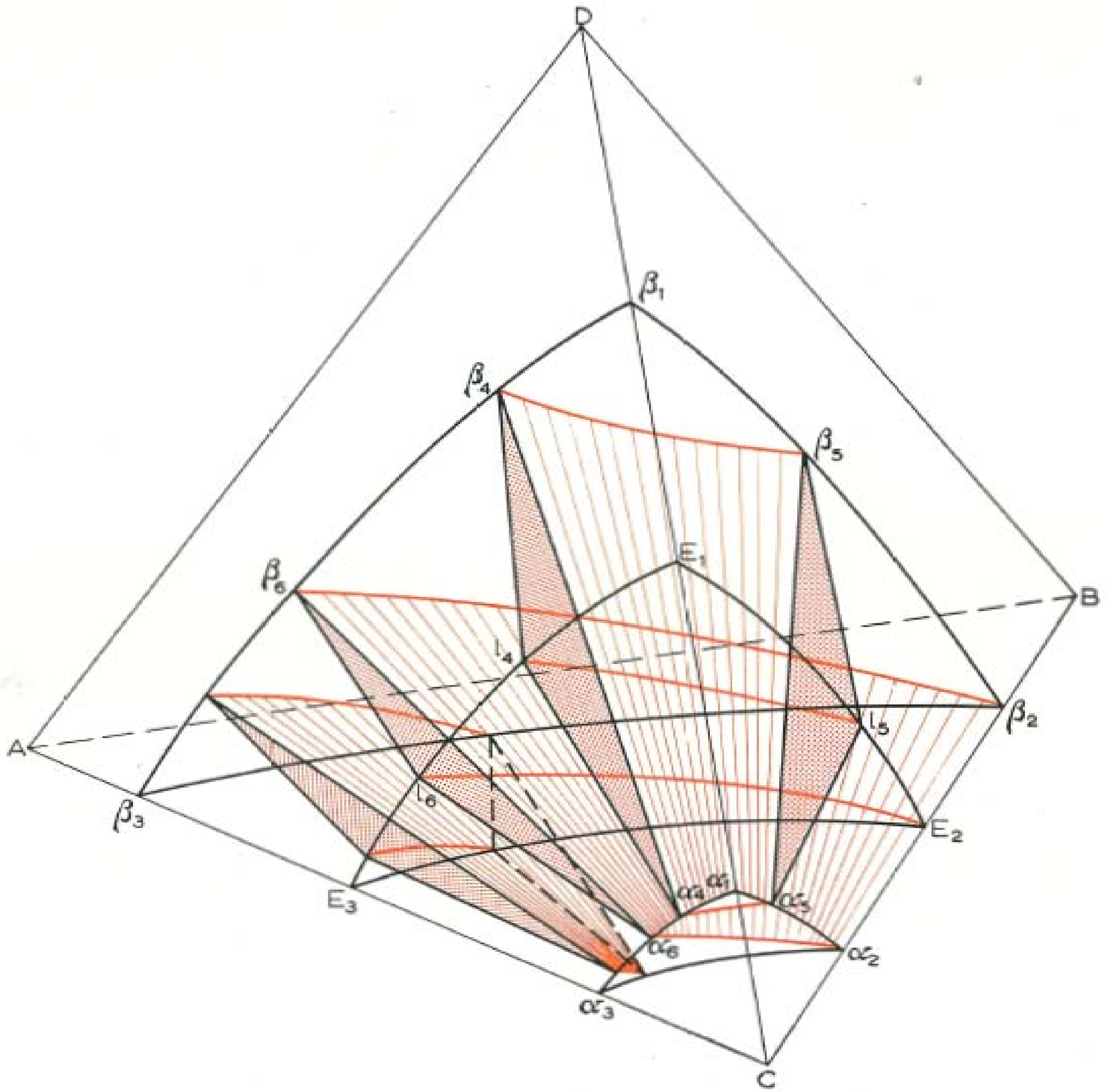

Fig. 255. Polythermal projection of a quaternary system involving three-phase equilibrium of the type l $\rightleftarrows \alpha + \beta$

$T_D > T_C > E_1 > T_B > T_A > E_2 > E_3$

* Binary eutectic: CA, CB, CD
& A, B, D form continuous series of binary solid solution with each other.

* Face *ACD* of the tetrahedron ABCD= polythermal projection of the ternary system ACD

: Continuous transition from the binary eutectic CD to the binary eutectic AC (monovariant liquidus curve E_1E_3)

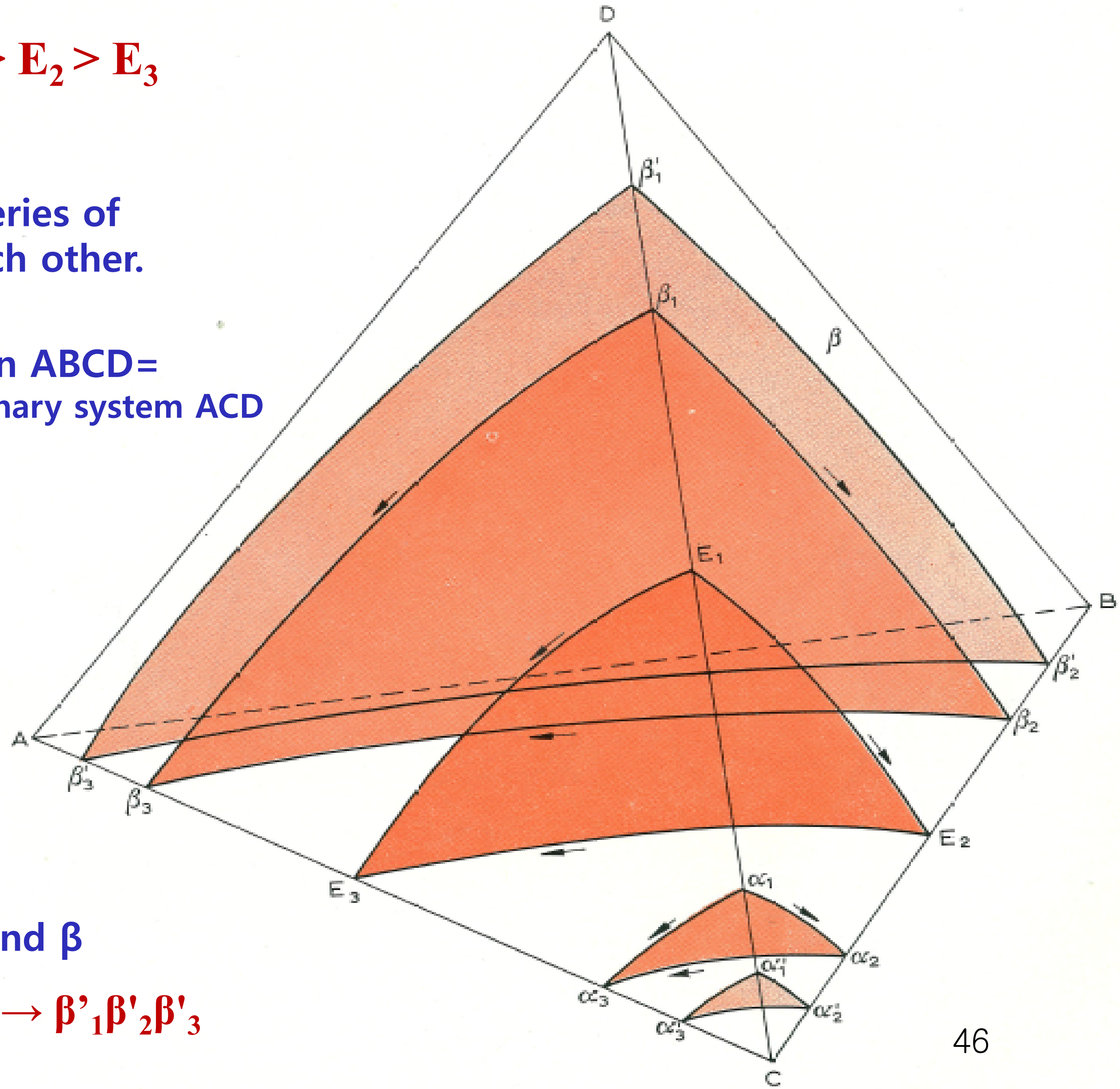

* Change in solubility in α and β

$\alpha_1\alpha_2\alpha_3 \rightarrow \alpha'_1\alpha'_2\alpha'_3$, $\beta_1\beta_2\beta_3 \rightarrow \beta'_1\beta'_2\beta'_3$

* Equilibrium freezing of alloys

A method proposed by Schrader and Hannemann

: the construction of a three-dimensional temperature-concentration section for a constant amount of one of the components.

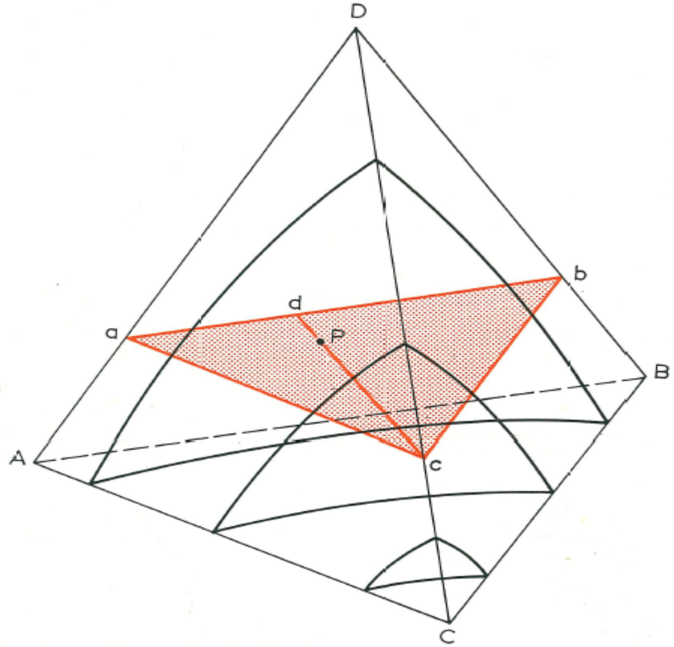

Fig. 258. Position of alloy *P* on plane *abc*.

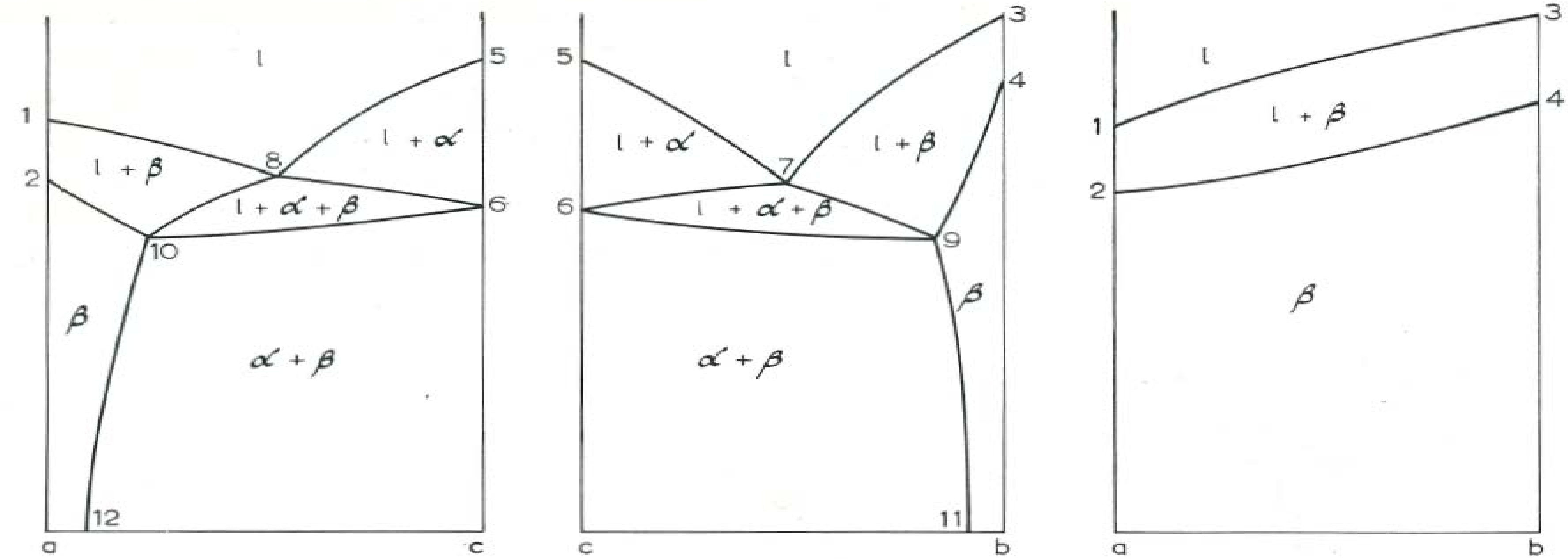

Vertical sections a-c, c-b, and a-b at the ternary faces ACD, BCD, and ABD

Fig. 260. (a) Three-dimensional temperature-concentration diagram for a quaternary system abc; (b) two-dimensional section throgh Fig. 260 (a).

*** Consider the solidification of alloy P on plane abc,**

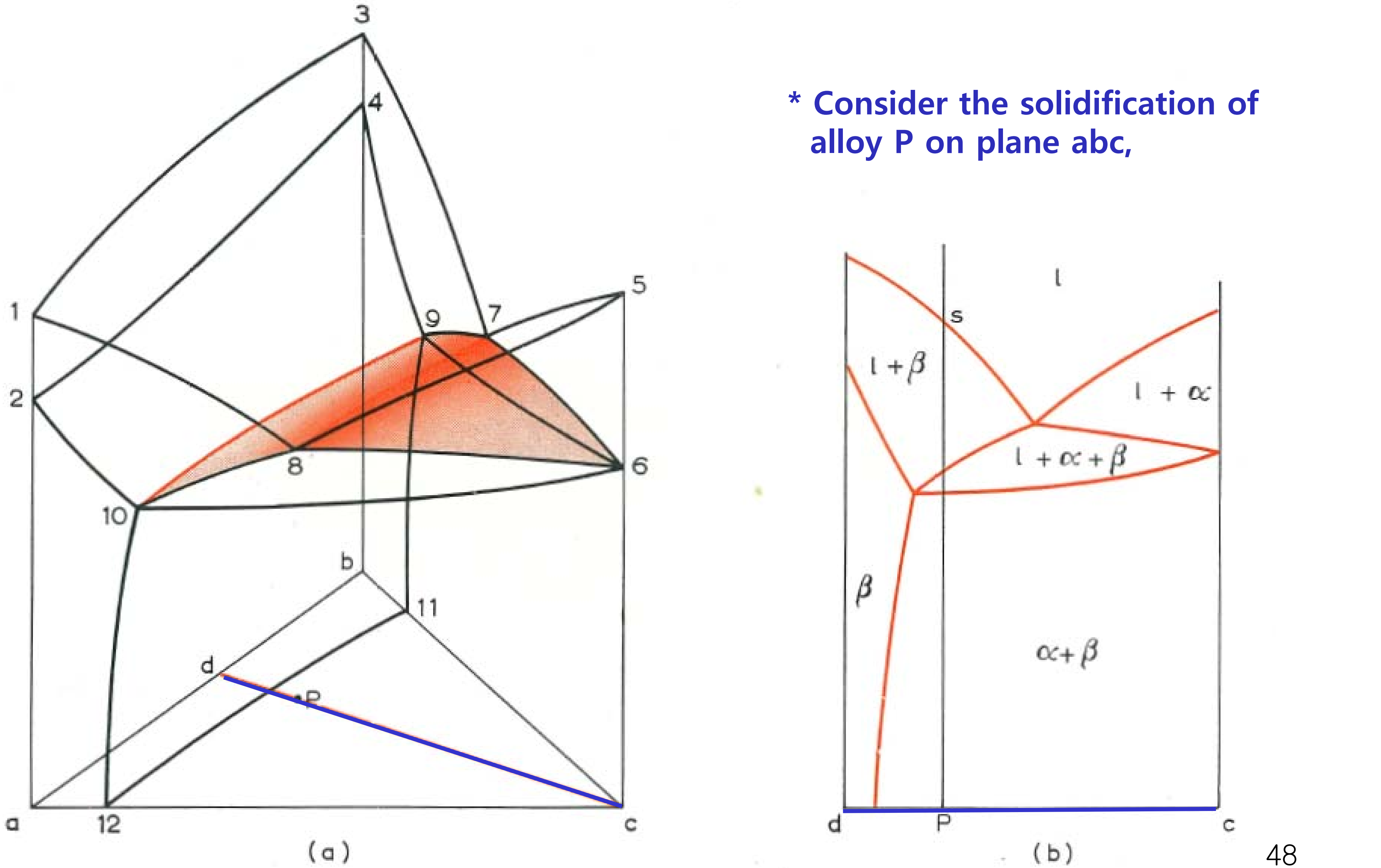

Fig. 261. Freezing of quaternary alloy P illustrated by reference to the polythermal projection of Fig. 255.

* Consider the solidification of alloy P

1) β solid solution precipitation with β_4 composition

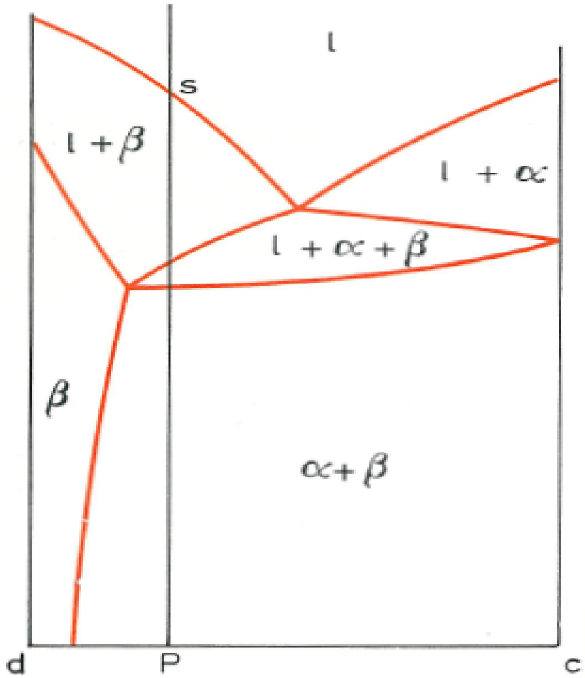

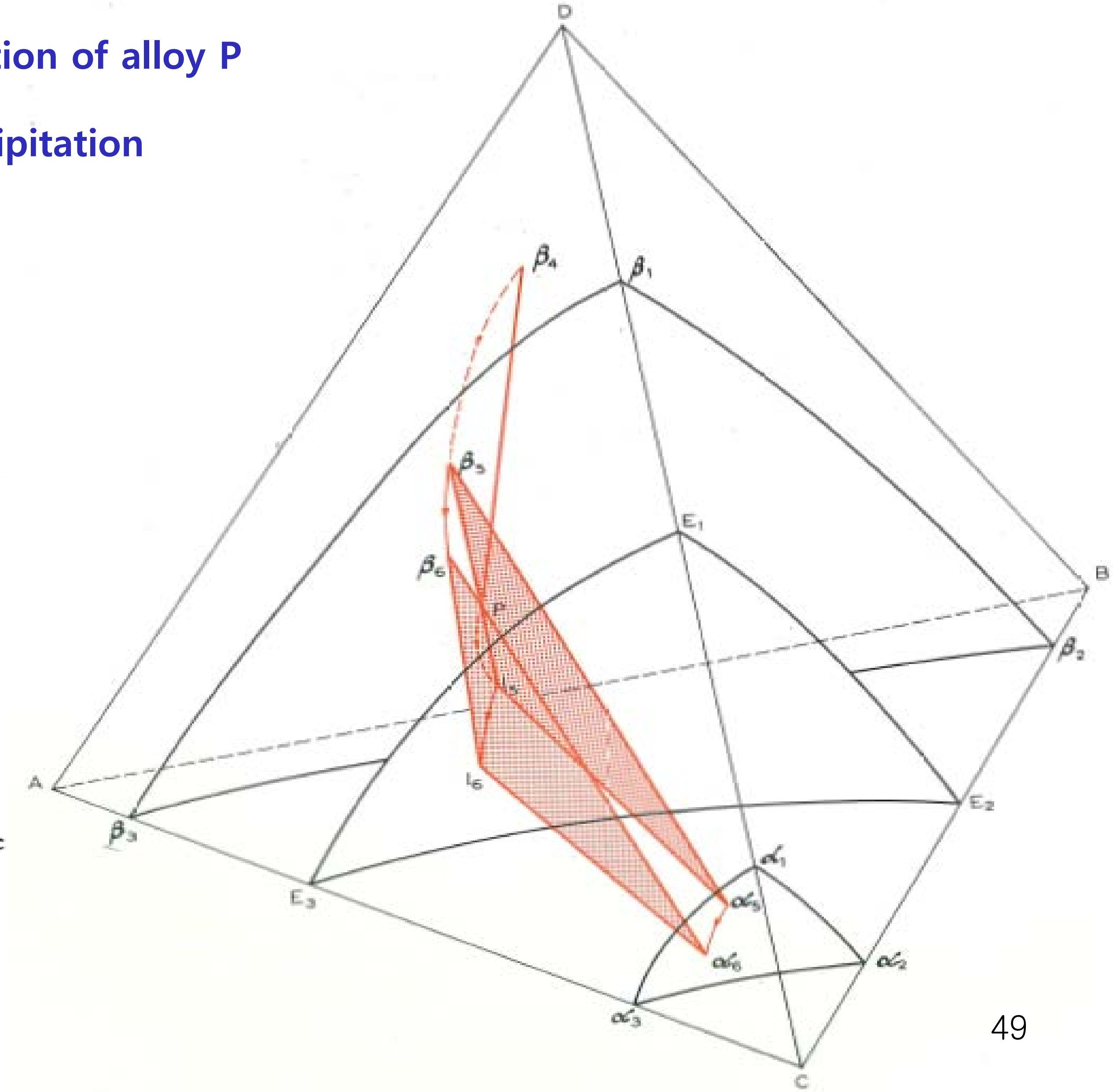

Fig. 261. Freezing of quaternary alloy P illustrated by reference to the polythermal projection of Fig. 255.

* Consider the solidification of alloy P
: primary (1) and secondary crystallization (3)

T ↓

1) β solid solution precipitation with β_4 composition

2) β phases trace paths similar to those shown in Fig. 253. ($\beta_4 \rightarrow \beta_5$)

3) Liquid meet the eutectic surface $E_1E_2E_3$.
$\rightarrow$ three phase equilibrium appear.
($l_5\alpha_5\beta_5 \rightarrow l_6\alpha_6\beta_6$)

4) With cooling to room temperature,
$\alpha_1\alpha_2\alpha_3 \rightarrow \alpha'_1\alpha'_2\alpha'_3$, $\beta_1\beta_2\beta_3 \rightarrow \beta'_1\beta'_2\beta'_3$